VAN ALLEN BELT PLASMA PHYSICS

C. F. Kennel and H. E. Petschek

RESEARCH REPORT 259
December 1966

AVCO EVERETT RESEARCH LABORATORY

A DIVISION OF AVCO CORPORATION

VAN ALLEN BELT PLASMA PHYSICS

by

C. F. Kennel and H. E. Petschek

AVCO EVERETT RESEARCH LABORATORY
a division of
AVCO CORPORATION
Everett, Massachusetts

December 1966

ABSTRACT

We review recent theoretical developments in understanding the
plasma turbulence in the Van Allen belts. More complex geophysical
turbulence phenomena, such as the auroral zone, are not explicitly
treated, since their theoretical description is still incomplete. In
particular, it now appears likely that instability, and the resulting quasi-
linear pitch angle scattering, in the so-called whistler and ion cyclotron
modes, limits the fluxes of energetic electrons and ions, respectively,
that can be stably trapped in the Van Allen belts, where the Earth's
magnetic lines have a dipole "mirror" configuration. We discuss semi-
quantitatively the factors which affect the stability of such waves propa-
gating obliquely to the local magnetic field direction, the velocity space
diffusion resulting from their nonlinear growth, and finally, some
observations relating to the Van Allen belt turbulence.

TABLE OF CONTENTS

1. Introduction

In this paper, we will discuss some aspects of plasma turbulence in the Van Allen belts, a small part of the overall complex of phenomena related to the Earth-Solar Wind Interaction. To put our discussion in perspective, we will first briefly outline the state of knowledge concerning the whole magnetosphere, and then focus our attention on the Van Allen belts.

Our knowledge of the Earth's near environment in space has grown tremendously in the last decade. The Earth's magnetic field, once thought to be a dipole extending in space to great distances, is now known to be greatly modified by interaction with the solar wind plasma flow. The Earth and its magnetic field present a blunt obstacle to the highly super-sonic solar wind flow. Just as in ordinary collisional gases, a shock wave stands upstream from the Earth (Ness, et al, 1964). However, the dissipation necessary to create the shock must arise from collisionless plasma turbulence processes, as yet imperfectly understood. The flow downstream from the shock is at least partially randomized in direction and energy distribution (Bridge, et al, 1965; Wolfe, 1966). The downstream magnetic field is highly turbulent (Ness, et al, 1964). The total pressure of the post-shock solar wind flow is sufficient to confine the Earth's magnetic field to a cavity, "the magnetosphere", whose dimensions are fixed by the balance of solar wind pressure to Earth dipole magnetic pressure. The transition layer between the post-shock solar wind and the magnetosphere appears to be quite thin (Cahill and Amazeen, 1963; Ness et al, 1964).

The Earth's lines of force are coupled to those of the solar wind by dissipation at the transition layer and are stretched into an extended magnetic tail on the downstream side of the Earth. Here a thin neutral sheet of low magnetic and high particle pressure has been observed (Ness, N.F. 1965; Bame, et al, 1966). The flow of relatively dense, hot plasma from the neutral sheet towards the Earth's night side is widely thought to be responsible for the complex phenomena occurring in the auroral zone (for instance, see Axford, et al, 1965 or O'Brien, 1966). The auroral zone is a highly turbulent region of intense energetic ($\approx$ 1keV) particle precipitation from the magnetosphere to the atmosphere on the Earth's night side, corresponding to equatorial plane distances greater than six Earth radii from the Earth. Here auroral arcs -- intense, spatially localized, sometimes unsteady precipitation events occur, superposed on the already high background level. No satisfactory theoretical explanation for these extraordinary events exists at this time.

We shall not cover in these lectures the many active areas of research concerning the structure of the magnetosphere so briefly mentioned here. Those so interested may turn to the extensive literature, (see, for instance, Levy, et al, 1964; Ness, 1966; Dessler and Juday, 1965; O'Brien, 1966). Rather we will concern ourselves with the Van Allen trapped energetic particle radiation found on lines of force deeper inside the magnetosphere, where the bulk interaction with the solar wind is less pronounced. This may be inferred from the fact that the magnetic lines of force retain their dipole topology and are only relatively weakly distorted from their unperturbed values. In this region of space, the Earth's magnetic field has a "mirror" configuration, similar to that in laboratory "mirror" confinement devices for thermonuclear fusion, and should trap particles.

The geometry of an idealized steady magnetosphere is illustrated in Fig. 1. Shown are the solar wind (1), the bow shock wave (2), the post-shock plasma flow (3), the magnetosphere boundary (4), the magnetospheric tail (5), the neutral sheet (6), the auroral zone (7), and the Van Allen Zone (8). The Van Allen Zone is often separated into an Inner and Outer Zone. We will not discuss the Inner Zone. In the quasi-dipole Van Allen region, geophysicists often characterize an entire tube of force and the radiation trapped on it by the distance L in Earth radii from the Earth's center to the intersection of the line of force with the geomagnetic equatorial plane. These are called L-shells, with $L \approx 3$ denoting that tube which has its intersection three Earth radii from the Earth, and so on. Henceforth, we will use this convenient terminology.

In keeping with the plasma turbulence motif of this institute, we will restrict our discussion to those turbulent plasma processes which may account for the observed anomalously large losses of protons and electrons ostensibly trapped in the Outer Van Allen Zone. In addition, we shall present, in an unnaturally linear fashion, primarily the course of research as it was pursued at the Avco Everett Research Laboratory and at the International Centre for Theoretical Physics, Trieste. Many of the ideas to be presented have been discussed previously by Dragt (1961), Wentzel (1963), Dungey (1963), Brice (1964), Cornwall (1964, 1965, 1966), Andronov and Trakhtengehrts (1964) and others. Our debt to these and other authors is hereby acknowledged. Since we will stress physical concepts and linearity of presentation, those readers who still hanker for more details should turn to the extensive literature. A theoretical discussion of the loss of ions from laboratory mirror machines, involving the "loss-cone instability" (Rosenbluth and Post, 1965; Post and Rosenbluth, 1966; Galeev, 1966), has recently been advanced. This is similar in many respects to the magnetospheric ideas to be presented, though the basic instabilities differ.
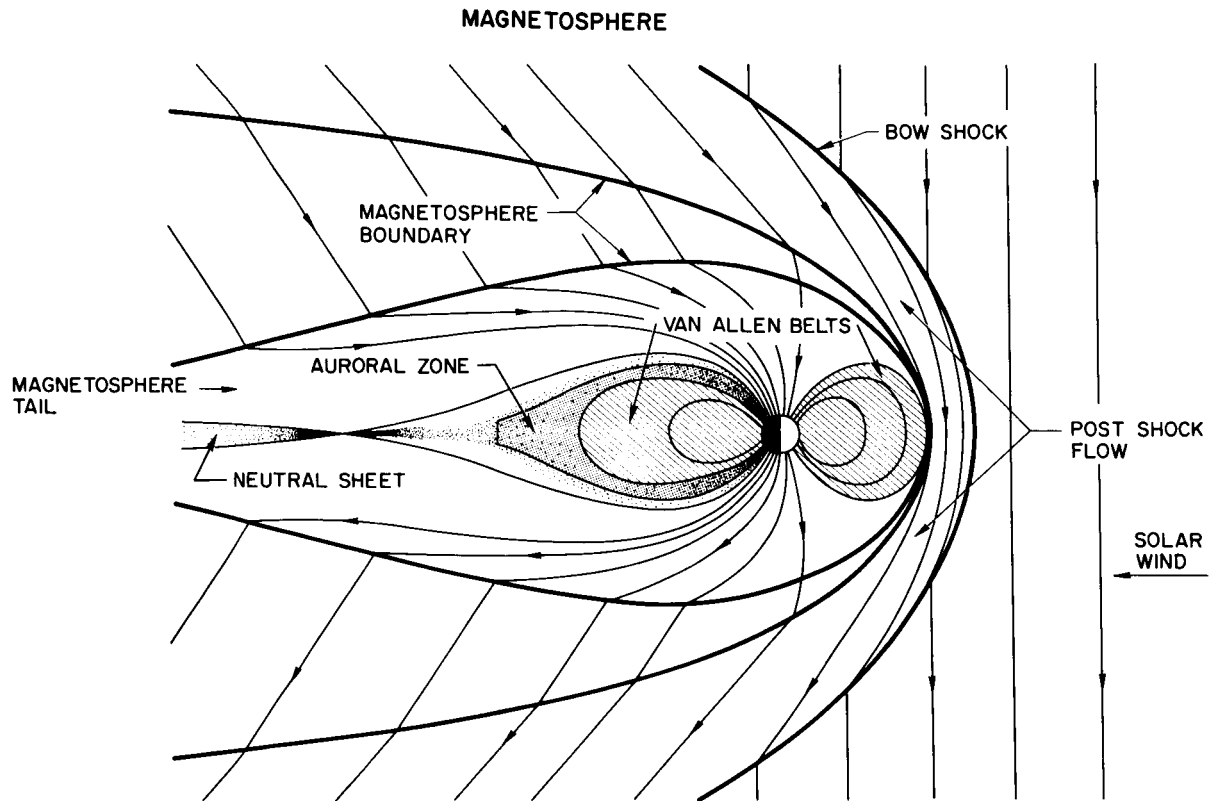
MAGNETOSPHERE

Fig. 1   Magnetosphere

This figure schematically summarizes our present knowledge of the Earth-Solar wind interaction. Shown is an idealized steady state magnetosphere. The magnetosphere boundary is split up into two discontinuities, corresponding to the standing waves which are part of the field annihilation region (where post-shock solar wind and Earth magnetic lines are connected) as in the theory of Levy, et al. (1964). Note the different locations of the auroral and Van Allen zones, considered to be distinct in this paper.

2. Van Allen Belt Observations

In this section, we present a selective review of those Van Allen Belt particle observations we have found useful for inferring the properties of the turbulence there. For more complete reviews of the observational literature, the reader may turn to Frank (1965), Brown (1966), O'Brien (1966), and others.

In the Van Allen Zone are large fluxes ($10^{7-8}/cm^2$-sec) of energetic electrons and protons which are at least quasi-tra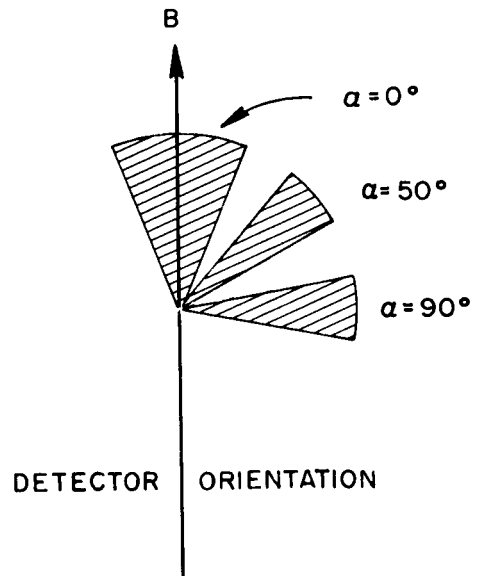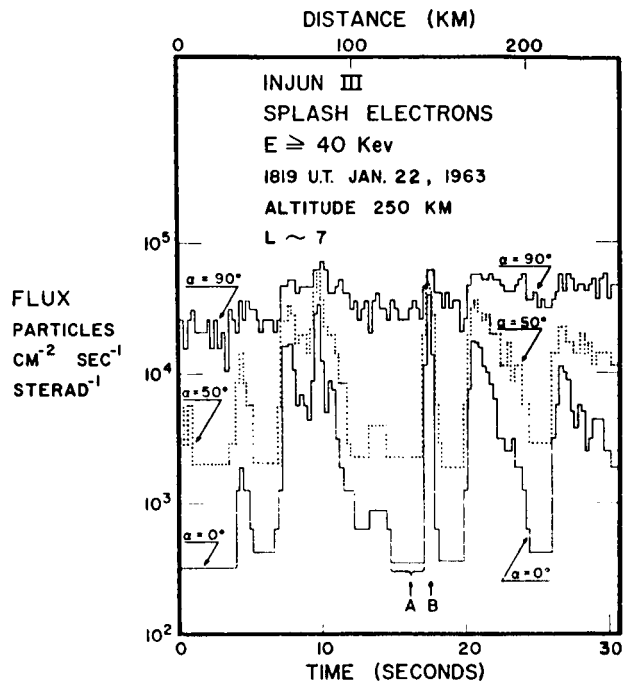pped on those lines of force which are topologically dipole. Most detectors of energetic electrons and protons have had energy thresholds of, say, a few tens of keV. Fortunately, this has been sufficient for the Van Allen Zone. Large fluxes ($\sim 10^9/cm^2$-sec) of much lower energy electrons, a few keV, have been observed in the auroral zone, just outside the Van Allen region. While the auroral and Van Allen regions seem intimately related (O'Brien and Taylor, 1964; O'Brien, 1966), it appears that a separate discussion of the Van Allen Zone may be feasible to lowest approximation, since particles of low ≈ 1 keV auroral energy are not observed in the Van Allen Zone.

The precipitation of energetic electrons from the Earth's magnetosphere to its atmosphere, long observed visually from the ground by the auroral light excited by electron impact, was first directly observed by detectors mounted on rockets and balloons (Van Allen, 1957; Winckler, et al, 1963; Anderson and Milton, 1964 and many others). Subsequently, surveys by the Alouette I (McDiarmid, et al, 1964) and Injuns I and III satellites (O'Brien, 1962, 1964) which circled the Earth in North-South orbits at altitudes near the electrons' mirror points, greatly increased our understanding of particle precipitation.

Figure 2 is a sample of the >40 keV electron fluxes measured by the near-Earth satellite Injun III (O'Brien, 1964) at various pitch angles α

DISTANCE (KM)

INJUN III
SPLASH ELECTRONS
$E \geqq 40$ Kev
1819 U.T. JAN. 22, 1963
ALTITUDE 250 KM
L ~ 7

FLUX
PARTICLES
CM^{-2} SEC^{-1}
$STERAD^{-1}$

TIME (SECONDS)

DETECTOR | ORIENTATION

O'BRIEN, JGR, 69, 1, 1964

Fig. 2   Injun III > 40 keV electron precipitation fluxes

Injun III was oriented with respect to the local magnetic
field direction. $\alpha = \pi/2$ signifies electrons mirroring
locally at the satellite. The $\alpha = 0°$ electrons are plunging
towards the atmosphere. $\alpha = 55°$ is an intermediate case.
Notice that there appears to be a precipitation background
throughout, that large, rapid fluctuations occur, during
which the electrons > 40 keV approach pitch angle isotropy
locally. All these electrons have small pitch angles in the
equatorial plane.

-6-

relative to the local magnetic field. The curves labelled $\alpha = 90^{\circ}$, measure electrons $\gtrsim 40$ keV with flat pitch angles which are locally mirroring and will be returned back towards the equatorial plane. These electrons are trapped. The $\alpha = 0^{\circ}$ detector measures small pitch particles with velocities directed along the magnetic field direction. These will be precipitated into the atmosphere. The $\alpha = 55^{\circ}$ electrons are an intermediate case. If the electrons observed conserve their first adiabatic invariant in their motion along the line of force between the Injun III satellite and the equatorial plane (an assumption to be shown theoretically reasonable), they all would have very small equatorial pitch angles.

Figure 2 is probably an exaggeratedly complex swath of data. (Our purpose in showing it is to instill a sense of humility in theorists.) Nevertheless, it does contain features which O'Brien (1964) has succeeded in showing hold more or less generally for all the >40 keV electron precipitation. Electrons >40 keV seem often to be precipitating into the atmosphere from the Outer Van Allen Belts. Injun I observations (O'Brien, 1962) of the electron precipitation rate together with estimates of the total number of energetic Van Allen electrons >40 keV trapped on a tube of force obtained independently by equatorial plane satellites enabled O' Brien (1962) to estimate the electron lifetime as 10^{3-5} seconds, i.e., twenty minutes to a day. >40 keV electron precipitation typically covers a range of L-shells bordered on its inner edge at $L \approx 2$ by the Inner Van Allen zone and at the outer edge at $L \approx 6-8$ by the auroral zone. Precipitation of energetic >40 keV electrons increases with increasing L and maximizes in the auroral zone (O'Brien, 1964; Gurnett and Fritz, 1965). The auroral light itself is thought to be due to the intense precipitation of other low energy electrons with a few keV energy (O'Brien and Taylor, 1964). Low energy auroral electron precipitation does not occur on Van Allen L-shells;

the Van Allen electrons have much higher energies but much smaller intensities than the auroral electrons. We will not discuss the auroral precipitation here.

Since the number of >40 keV electrons observed in the Van Allen Belts over many years has never fallen to zero, and since precipitation seems often, if not always, to occur, there must be active acceleration mechanisms maintaining the trapped >40 keV fluxes. What those mechanisms could be is a subject of active investigation in the research literature. O'Brien (1966) has adduced arguments that at least one such mechanism lies in the auroral zone. We will find that the precipitation of particles, while strongly coupled to the rate of acceleration to energies above the detector threshold, can be understood, in its broad outlines, without reference to the specific details of the acceleration mechanisms. Therefore, we will henceforth neglect to a first approximation both specific acceleration mechanisms and/or the poorly understood interaction between the auroral and Van Allen Zone, and consider the more well-defined problem of the loss of particles from the Earth's quasi-dipole field.

Figure 2 illustrates that the $a = 0^{\circ}$ precipitation fluxes of electrons ≥ 40 keV undergo violent fluctuations of order 10^2 in time scales of one second. Anderson and Milton, (1964), Mozer et al, 1965, Mozer and Bouston, 1966, have observed precipitation rate fluctuations in time scales as short as 0.1 seconds. From these short time scales we can induce arguments about the precipitation mechanism. In the absence of fluctuating fields, the particles should conserve their adiabatic invariants. These are, in order of increasing stringency:

(a) The total magnetic flux contained in one complete guiding center drift orbit about the Earth -- the so-called third invariant. Fluctuations of the order of the guiding center drift period around the Earth (a few thousand seconds) are needed to violate this invariant.

(b) the longitudinal invariant $J = \int_{-\ell_1}^{+\rho} v_{\shortparallel} \, d\ell$, where $d\ell$ is an element of length along the line of force, $v_{\shortparallel}$ the parallel velocity component and $\pm\ell_1$, the mirror points. Fluctuations with time scales the order of the particle bounce period between mirror points, a few seconds, are needed for violation.

(c) the magnetic moment or first invariant $\mu = \dfrac{\sin^2 \alpha}{B}$, where α is the pitch angle and B the magnetic field strength. Gyro-period fluctuations, $\sim 10^{-4}$ seconds in the equatorial plane and faster elsewhere along a line of force, will violate this invariant. Particle acceleration and precipitation can result from violation of any of these invariants. For a review of the geophysical consequences of second and third invariant violations, see Dungey (1965).

Suppose that precipitation is due to a velocity-space diffusion process, a currently popular hypothesis in plasma physics. Then fluctuations in each range of characteristic period will cause the particle distributions to diffuse slowly in adiabatic invariant velocity space. Generally speaking, it would take several of the basic periods outlined above for the diffusion from a given adiabatic invariant violation to be effective. It is therefore difficult to associate second and third invariant violation with the 0.1-1 second fluctuations in precipitation rate. This leads us to first invariant violation.

McDiarmid and Budzinski (1964) noted that the fluxes of electrons >40 keV and their distribution with energy observed both in the vicinity of the equatorial plane and near the mirror points near the Earth are quite similar. If electrons conserve their first invariant as they change from trapped to precipitated by penetrating regions of ever increasing magnetic field strength in going from equatorial to high latitude mirror points, they

would acquire an enormous energy. This energy gain would be hard to reconcile with the observed spectral similarities. This suggests:

(a) The first adiabatic invariant is violated.

(b) Electron pitch angles must change much more than their energy in the precipitation process.

That it is primarily the pitch angle and not the energy which changes during electron precipitation is suggested from the tendency shown in Fig. 2 and cited in many instances by O'Brien (1964), for the overall fluxes to approach pitch angle isotropy at least near the loss cone when the precipitation rate is high. Thus, the parallel electron motion is not significantly energized relative to the perpendicular. When the $\geqslant 40$ keV precipitation rate is extremely high, for instance, outside the Van Allen Zone on auroral lines of force, the precipitated flux is comparable with the trapped fluxes measured in the equatorial plane. From this we infer that the entire pitch angle distribution becomes roughly isotropic when precipitation is rapid.

Proton precipitation is much more difficult to detect. However, Haerendel (1966), after a study of the fluxes of trapped energetic proton fluxes observed by Davis and Williamson (1963), has concluded that first invariant violation is also necessary for protons. While we will bias our discussion in terms of electrons, there is an entirely similar discussion for proton precipitation. Moreover, since the trapped proton energy density observed in space is much larger than that for electrons, protons are actually the dominant component of the Van Allen belts.

3. Linear Pitch Angle Anisotropy Instabilities in the Magnetosphere

3.1) Introduction

In this section, we discuss instabilities in those electromagnetic plasma waves which can violate the first adiabatic invariant. For a system as complicated as the magnetosphere, evaluating even imprecisely the factors affecting its stability properties is, unhappily, complex. However, a good understanding of these factors is necessary for the interpretation of experiments.

The conditions for first adiabatic invariant violation are quite stringent. A particle must see fluctuating wave fields near its own gyro-frequency. The wave-particle interaction is particularly strong when it is resonant, i.e., when the relative phase of particle and wave changes slowly with time, so that the resonant particle feels the wave force for a long time. Here there can be an energy exchange between particle and wave. On the other hand, the forces between waves and non-resonant particles average to zero. In plasmas with an external magnetic field, we are led to the cyclotron resonance wave-particle interaction, where the free particle motion parallel to the external field Doppler shifts the wave frequency to the particle's gyrofrequency. The condition for this resonance is

$$V_{||} = \frac{\omega - \Omega_{\pm}}{K_{||}} \tag{3.1}$$

where $V_{||}$ is the particle velocity component parallel to the field, $K_{||}$ the parallel wave number, ω the wave frequency, and $\Omega_{\pm}$ the gyrofrequency for ions (+) or for electrons (-). Since there can also be resonances at harmonics of the gyrofrequency, we distinguish this "lowest" resonance from the others by calling it the principal cyclotron resonance.

In the following, we will consider the cyclotron resonance couplings of whistlers to electrons and of ion cyclotron waves to protons. In 3.2, we discuss the special case of couplings to those waves which propagate strictly along the magnetic field. Here we show that the Van Allen electrons and protons have the appropriate energy to be in cyclotron resonance with whistlers and ion cyclotron waves, respectively. Furthermore, the cyclotron resonance interaction causes parallel propagating waves to grow when the particle pitch angle distributions have a mirror type pitch angle anisotropy, with more energy in motion perpendicular to the field than in parallel. In 3.3, we argue that whistlers as they propagate must change their wave normal angles to the magnetic field, necessitating the consideration of the much more complex linear instability problem for obliquely propagating waves, which is then outlined in 3.4. The ray path and instability calculations are combined in 3.5. Here we conclude that growth along a ray path will occur when the trapped low energy particle fluxes are sufficiently weak. In 3.6, we account schematically for other non-resonant losses of wave energy from the magnetosphere.

3.2) Parallel Propagating Whistlers and Ion Cyclotron Instabilities

As a first approximation, assume that the real part ω of the wave frequency is given by the cold plasma dispersion relation (Stix, 1962; Allis, et al, 1963). Then using 3.1, we may estimate the energy of resonant particles and compare with observed Van Allen particle energies. The ion cyclotron wave is a left-hand circularly polarized electromagnetic wave with a frequency below the ion gyrofrequency Ω_+, and a cold-plasma dispersion relation

$$\frac{\omega^2}{K^2} = V_A^2 \left(1 - \frac{\omega}{\Omega_+}\right) \qquad (3.2)$$

where $V_A = B/(4\pi N M_+)^{1/2}$, the Alfven velocity, M_+ is the ion mass, and N the total electron or ion number density. Since $0 < \omega/\Omega_+ < 1$, the ion cyclotron wave propagates slower than the Alfven speed.

The whistler is a right hand circularly polarized electromagnetic wave with a frequency above the ion gyrofrequency, Ω_+, and below the electron gyrofrequency, $\Omega_- = -eB_0/M_- C$. When $|\omega/\Omega_-| \ll 1$, the cold plasma dispersion relation is

$$\frac{\omega^2}{K^2} = V_A^2 \frac{\omega}{\Omega_+} \tag{3.3}$$

Since $\omega/\Omega_+ > 1$, whistlers propagate faster than the Alfven speed. Combining (3.2) and (3.3) with (3.1), we can estimate the energy in parallel motion necessary for principal cyclotron resonance.

$$E_R^\pm = \frac{1}{2} M_\pm \left(\frac{\omega - \Omega_\pm}{K_{\shortparallel}}\right)^2 \tag{3.4}$$

In addition to the principal and higher cyclotron resonances discussed above, there can also be a resonance when the particle motion parallel to the magnetic field keeps up with the wave phase motion. The resonance condition for the "Landau" resonance is

$$V_{\shortparallel} = \omega/K_{\shortparallel} \tag{3.5}$$

and the energy in parallel motion necessary for resonance is $1/2\, M_\pm (\omega/K_{\shortparallel})^2$.

While the Landau resonance is dominant for purely electrostatically polarized waves propagating along the magnetic field, there is no Landau resonance for parallel electromagnetic waves. The Landau effects, which occur only for obliquely propagating electromagnetic waves, will be discussed in section 3.4. However, we list the Landau energies in Table I for completeness.

TABLE I

RESONANT ENERGIES

	Ion Cyclotron Wave	Whistler Mode
Cyclotron Electrons	$\gtrsim \dfrac{M_+}{M_-} \dfrac{B^2}{8\pi N}$	$\dfrac{|\Omega_-|}{\omega} \dfrac{B^2}{8\pi N}$
Cyclotron Ions	$\approx \dfrac{B^2}{8\pi N} \left(\dfrac{\Omega_+}{\omega}\right)^2$	$\dfrac{M_+}{M_-} \dfrac{B^2}{8\pi N}$
Landau Electrons	$\approx \dfrac{B^2}{8\pi N} \dfrac{M_-}{M_+}$	$\dfrac{\omega}{|\Omega_-|} \dfrac{B^2}{8\pi N}$
Landau Ions	$\approx \dfrac{B^2}{8\pi N}$	$\dfrac{M_+}{M_-} \dfrac{B^2}{8\pi N}$

The resonant energies for electromagnetic waves all scale with respect to $B^2/8\pi N$, the magnetic energy per particle in equilibrium. Since $B^2/8\pi$ increases rapidly approaching the Earth along a line of force, $B^2/8\pi N$, and therefore resonant particle energies, will be a minimum in the equatorial plane for any given line of force. A given wave will, therefore, encounter the greatest number of particles with energies appropriate for resonance when it propagates through the equatorial plane. Since resonant particle growth rates depend upon the number of resonant particles, the largest increment of resonant growth or damping will occur there. Therefore, it is appropriate to ask whether the observed >40 keV electrons and >100 keV protons have energies permitting cyclotron resonance with the whistler and ion cyclotron waves, respectively, in the equatorial plane.

The magnetic energy per particle, $B^2/8\pi N$, in the equatorial plane is plotted as a function of radial distance in Fig. 3. The magnetic field was

taken to be that of a dipole plus small distortions due to the interaction
with the solar wind. These amounted to including a small day-side solar
wind compression and a small night-side decompression from the stretched
out magnetospheric tail. The equatorial plane electron number density
variation was estimated by Carpenter and Smith (1964). The details of
Fig. 3 are probably not significant; moreover, $B^2/8\pi N$ probably varies
with time, especially during magnetic storms. However, the rough order
or magnitude indicated by Fig. 3 for $B^2/8\pi N$, establishes that whistlers
and ion cyclotron waves, with frequencies well below the appropriate gyro-
frequency in the equatorial plane, do have cyclotron resonances with the
observed Van Allen electrons and protons. For instance, at $L = 4$,
whistlers with $|\omega/\Omega_-| \approx 1/20$ cyclotron resonate with ≈ 40 keV electrons, and
$\omega/\Omega_+ \approx 1/7$ ion cyclotron waves resonate with ≈ 100 keV protons.

While other resonances do not affect parallel propagating electro-
magnetic waves, they are important for obliquely propagating waves.
For instance, in section 3.4, we will argue that Landau resonance particles
tend to damp obliquely propagating waves. For the $|\omega/\Omega_-| \approx 1/20$ whistler at
$L \approx 4$, Table I and Fig. 3 indicate that the Landau electrons have roughly
50-100 eV energy, and are therefore quite significant, whereas Landau
protons will have a few meV and are probably unimportant. For the
$\omega/\Omega_+ \approx 1/7$ ion cyclotron wave, Landau ions have ≈ 2 keV and Landau
electrons, ≈ 1 eV. In section 6, we will argue that higher cyclotron
resonance interactions at multiples of the gyrofrequency, given by the
condition $K_{||} V_{||} = \omega - n\Omega_{\pm}$, can be responsible for the slow precipitation of
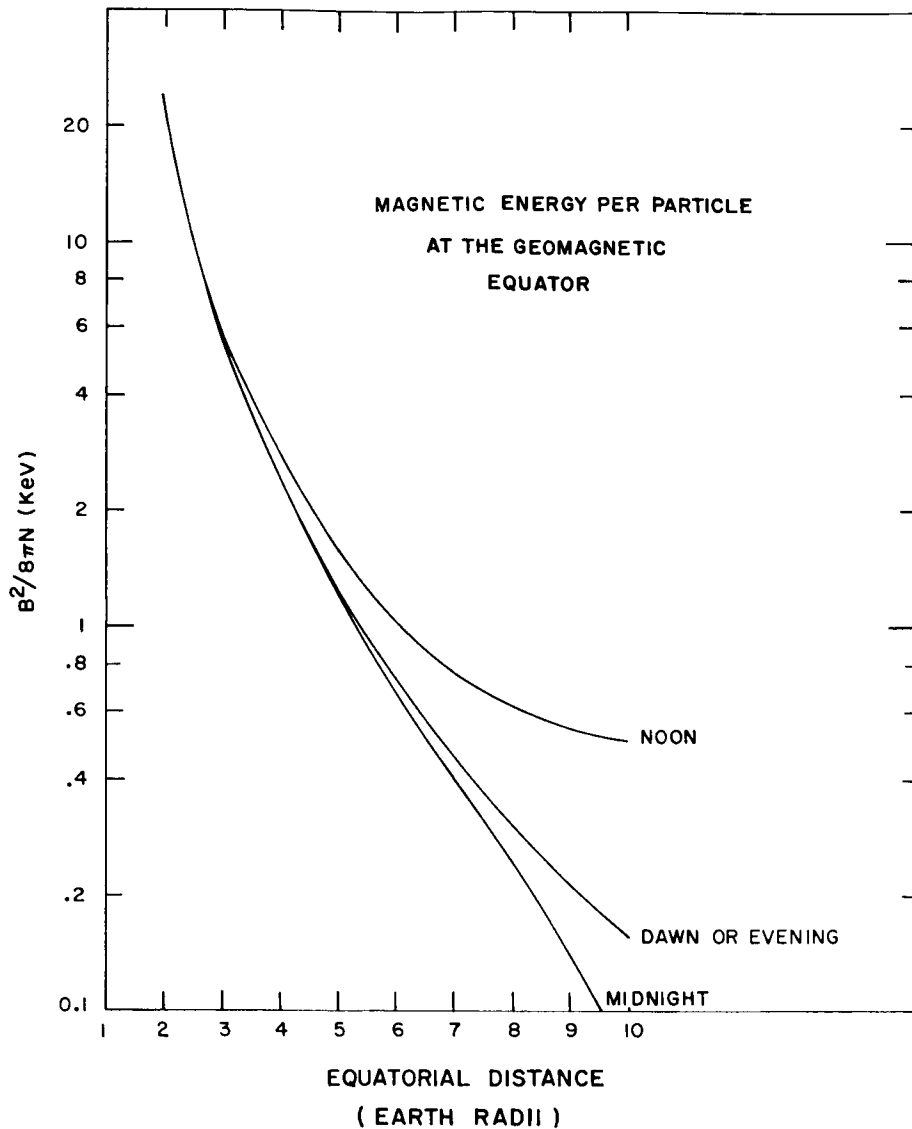
Fig. 3   Equatorial Plane Magnetic Energy per Particle

Shown here are rough estimates of $B^2/8\pi N$, which determines resonant particle energies for electromagnetic waves for the equatorial plane. $B^2/8\pi N$ probably increases rapidly away from the plane. This plot is based on idealized estimates of the magnetic field strengths, including the diurnal magnetic field distortion due to the solar wind (Kennel and Petschek, 1966) and electron densities given by Carpenter and Smith (1964).

high energy (200-400 keV) electrons. When $|\omega/\Omega_{\pm}| \ll 1$, the higher cyclotron resonant energies are just a factor n^2 larger than the basic $|n| = 1$ cyclotron energies listed in Table I.

For the present, we restrict our attention to parallel propagating whistlers and ion cyclotron waves, for which only the $|n| = 1$ principal cyclotron resonances occur. Formulae for the growth rates were first derived by Sagdeev and Shafranov (1961), and subsequently by numerous authors. For the low frequency whistler mode with $|\omega/\Omega_-| \ll 1$, the growth rate can be written schematically as follows, neglecting the small damping from few meV cyclotron protons:

$$\gamma \approx \Omega_- \, \eta^- \left\{ A^- - |\omega/\Omega_-| \right\} \tag{3.6}$$

where η^- and A^- will be defined shortly. $\gamma > 0$ denotes instability. Similarly, neglecting the small damping from few meV cyclotron electrons, the growth rate for the low frequency $\omega/\Omega_+ \ll 1$ ion cyclotron wave is roughly,

$$\gamma \sim \Omega_+ \, (\frac{\Omega_+}{\omega}) \, \eta^+ \left\{ A^+ - \omega/\Omega_+ \right\} \tag{3.7}$$

$A^{\pm}$ is a measure of the anisotropy of the pitch angle distribution of resonant particles,

$$A^{\pm} = \frac{\int d^3 v \, \frac{V_\perp}{2 V_{\shortparallel}} \, (V_{\shortparallel} \frac{\partial f^{\pm}}{\partial V_\perp} - V_\perp \frac{\partial f^{\pm}}{\partial V_{\shortparallel}}) \, \delta \, (V_{\shortparallel} - \frac{\omega - |\Omega_{\pm}|}{K_{\shortparallel}})}{\int d^3 v \, f^{\pm} \, \delta \, (V_{\shortparallel} - \frac{\omega - |\Omega_{\pm}|}{K_{\shortparallel}})} \tag{3.8}$$

where $\int d^3v$ denotes integration over velocity space, $V_\perp$ and $V_{\shortparallel}$ are velocity components perpendicular and parallel to the magnetic field respectively, and $f^\pm(V_\perp, V_{\shortparallel})$ is the equilibrium velocity distribution. By transforming to pitch angle α coordinates, with $\alpha = \tan^{-1} V_\perp/V_{\shortparallel}$, (3.8) may be written in a form which emphasizes the dependence upon gradients in the pitch angle distribution.

$$A^\pm = \frac{\int d^3v \, (\frac{\tan \alpha}{2} \, \frac{\partial f^\pm}{\partial \alpha}) \, \delta(V_{\shortparallel} - \frac{\omega - |\Omega_\pm|}{K_{\shortparallel}})}{\int d^3v \, f^\pm \delta (V_{\shortparallel} - \frac{\omega - |\Omega_\pm|}{K_{\shortparallel}})} \tag{3.9}$$

$A^\pm$ is positive for mirror-type pitch angle distributions, which have more energy in motion perpendicular than parallel to the magnetic field. Instability occurs, for the appropriate mode, when

$$A^\pm > \left| \frac{\omega}{\Omega_\pm} \right| \tag{3.10}$$

Thus, very small pitch angle anisotropies in the high energy particles, which resonate with low frequency $\omega/|\Omega_\pm| \ll 1$ waves, lead to the unstable growth of those low frequency waves.

On the other hand, the magnitudes of the growth rates are proportional to $\eta^\pm$, roughly the fraction of the total distribution near cyclotron resonance.

$$\eta^\pm = \frac{|\Omega_\pm| - \omega}{K_{\shortparallel}} \int d^3v \, f^\pm \, \delta (V_{\shortparallel} - \frac{\omega - |\Omega_\pm|}{K_{\shortparallel}}) \tag{3.11}$$

While the anisotropy needed for instability decreases when $\omega/\Omega_\pm \to 0$, so also in general does $\eta^\pm$, the fast particle intensity, since distributions ordinarily

fall off with increasing energy. When the fast cyclotron particle intensity is large, whistlers and ion cyclotron waves can have appreciable growth rates, even when the pitch angle anisotropy is small.

To summarize, when the whistler frequency is well below the electron gyrofrequency, and the ion cyclotron frequency is well below the ion gyrofrequency, small mirror-type pitch angle anisotropies of order $\left| \omega/\Omega_{\pm} \right|$, of the electrons and protons in cyclotron resonance destabilize respectively the whistler and ion cyclotron waves propagating parallel to the magnetic field. By contrast, when the wave frequencies are close to the particle gyrofrequencies, large anisotropies are required to produce instability. The lower the wave frequency relative to the appropriate gyrofrequency, the higher energy an ion or electron needs for cyclotron resonance. Since the growth rate is proportional to the fraction of the distributions of particles with velocities appropriate to cyclotron resonance, plasmas with high energy "tails" to their velocity distributions will be particularly susceptible to whistler and ion cyclotron wave growth.

3.3) Wave Propagation in the Magnetosphere

From section 3.2, those whistlers and ion cyclotron waves propagating nearly parallel to the magnetic field as they traverse the equatorial plane should increase their amplitude. On the other hand, since the magnetosphere is a spatially inhomogeneous propagation medium, it is likely that the waves as they propagate change their wave normal angles to the magnetic field. Then, the use of the instability formulae derived above for parallel propagation might be invalid, necessitating the consideration of the complicated oblique

propagation instability problem. We calculate the rate of change of the whistler wave normal angle along a ray path and discuss the related ion cyclotron wave problem in this section.

The cold plasma quasi-longitudinal approximation for the whistler index of refraction, $n^2 = C^2 K^2/\omega^2$, is (Allis, et al, 1963)

$$n^2 = \frac{C^2}{V_A^2} - \frac{\Omega_+}{\omega \cos\Theta} \tag{3.12}$$

C is the velocity of light and Θ the wave normal angle to the magnetic field. n^2 is proportional to $N/|B|\cos\Theta$ and becomes very large for strongly oblique propagation ($\cos\Theta$ small). When $\cos\Theta$ approaches $\omega/\Omega_-(\ll 1)$, (3.12) breaks down. We will use this index of refraction to calculate whistler ray paths. To do this, we must know the spatial distribution of N and $|B|$.

For simplicity, we choose $|B|$ to be given by that of an ideal magnetic dipole. A proper spatial variation of the electron density is somewhat more difficult to define. By measuring the dispersion of lightning generated whistlers, Carpenter and Smith (1964), Angerami and Carpenter (1966) and others have shown that $N/|B|$ is roughly constant in the equatorial plane. However, their method does not accurately estimate the density variation along the lines of force. A particularly simple choice is to take N constant along the lines, as in isothermal magnetostatic equilibrium. Using this idealized density distribution, Thorne and Kennel (1966) computed the ray paths. However, it is more interesting to plot the wave normal angle Θ against geomagnetic latitude λ as in Fig. 4.

As an aid to understanding Fig. 4, suppose temporarily that the magnetic field is straight, pointing in the z-direction. Then the differential equation for the rate of change with z of wave normal angle Θ is
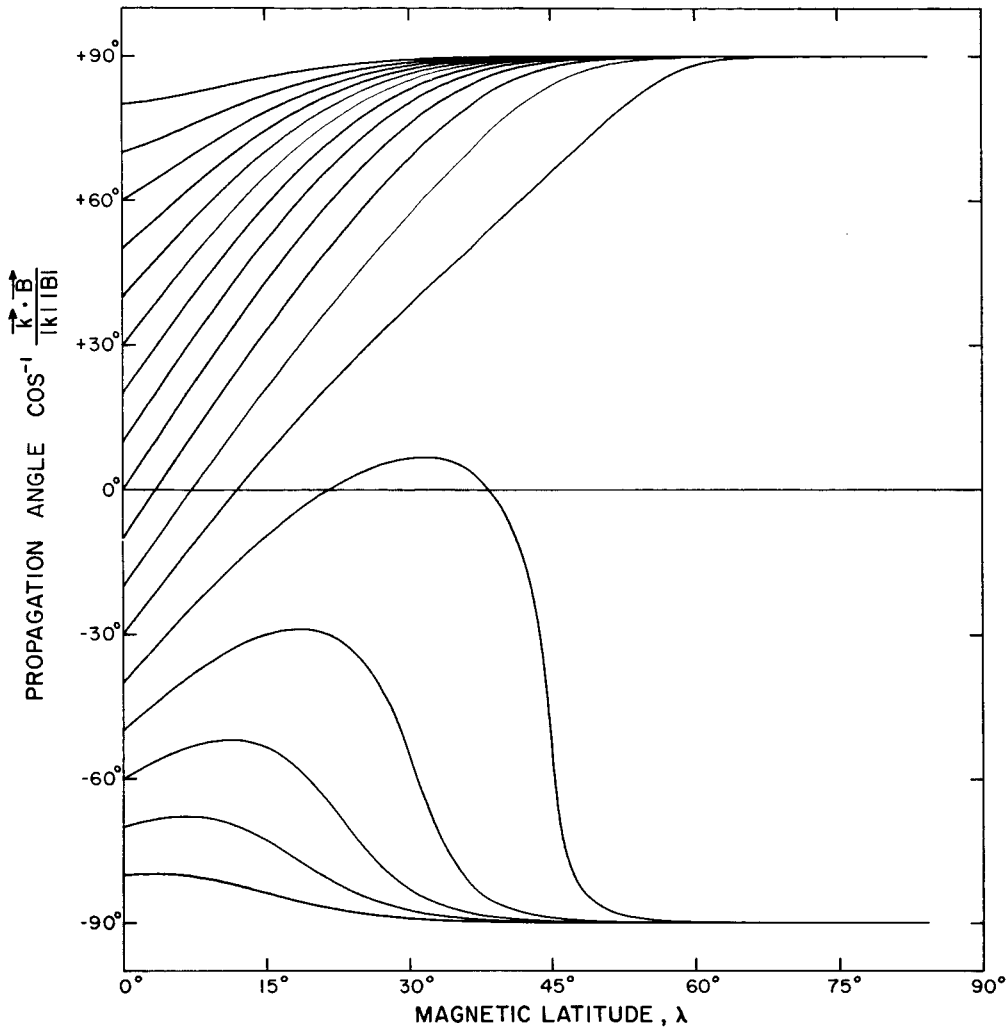
Fig. 4   Whistler Wave Normal Rotation

Plotted here is the variation of the wave normal angle Θ to be local magnetic field direction with geomagnetic latitude λ along a ray path in a meridian plane using the idealized density and magnetic field distributions of Thorne and Kennel (1966). $\Theta < 0$ denotes waves pointing towards the Earth, and vice versa for $\Theta > 0$. The waves thought to be most unstable, with $\Theta \approx 0°$ at $\lambda \approx 0$o, reach large wave normal angles at relatively low latitudes. The whistlers in the singular region at $\Theta \approx -30°$, $\lambda = 0$, first are rotated somewhat towards the field, but then, finally, away also. Even if N/B should be constant along a line of force, a significant fraction of the waves would reach large wave normals, simply because the Earth's magnetic field changes its direction in space.

-21-

$$\frac{d\Theta}{dz} = -\frac{d}{dz} \ln \; N/|B| \frac{\tan \Theta}{\tan^2 \Theta + 2} \tag{3.13}$$

When $N/|B|$ decreases along the ray path, as should occur for the magnetosphere, (3.13) indicates that waves rotate away from the magnetic field. Intuitively speaking, waves move into regions of increasing index of refraction; since $N/|B|$ decreases, they can only do so by decreasing $\cos \Theta$. When the magnetic field is curved, the rotation of the magnetic field direction as the wave propagates must be added to the rotation of the wave normal angle due to refraction as above. Those waves with initial angles $\Theta > 0°$ point away from the Earth; as they propagate they would normally increase their angle to the field, and an anisotropic refraction only enhances this effect. They reach large Θ rather quickly. Some of the waves with $\Theta < 0°$, pointing initially towards the Earth, decrease their wave normal angles for a while before they too are refracted towards large wave normal angles.

Some lightning-generated whistlers observed from the ground are thought to be "ducted", that is, contained in field aligned density striations which do not permit wave normal rotation. (See Helliwell, 1965 and Liemohn, 1966). These have been excluded from consideration. It does not seem likely that ducted radiation can play much of a role in a turbulence which must not be localized in order to fit the precipitation observations. Figure 3 suggests that unducted whistlers rapidly increase their wave normal angles, until at middle latitudes, $\lambda \approx 45°$, nearly all of them have their wave-vectors perpendicular to the local magnetic field direction.

We have not considered in detail the propagation of ion cyclotron waves in the magnetosphere. However, we do expect the wave normal angles

to rotate here as well, since the ion cyclotron index of refraction is also anisotropic.

$$n^2 = \frac{c^2}{v_A^2 \cos^2 \theta} \quad \alpha \quad \frac{N}{B^2 \cos^2 \theta} \tag{3.14}$$

We conclude therefore that both unducted whistlers and ion cyclotron waves can rapidly change their wave normal angles to the magnetic field. The serious question therefore arises whether the instability described by the parallel propagation analysis of 3.2 holds over a sufficient length of the ray path to ensure instability overall. The instability of obliquely propagating waves will be taken up in 3.4. In addition, the presence of ions drastically affects the index of refraction of whistlers propagating nearly normal to the magnetic field when the whistler frequency is close to the lower hybrid resonance (LHR) frequency

$$\omega \sim \omega_{LHR} \approx (\Omega_+ |\Omega_-|)^{1/2} . \tag{3.15}$$

In 3.6, we will suggest that both mode conversion and reflection can take place at the lower hybrid resonance.

3.4) Resonantly Unstable Off-Angle Electromagnetic Waves

We are forced to consider the instability of obliquely propagating waves. A general formula for the linear resonant growth rate of arbitrary wave modes in terms of the wave polarizations has been derived by Kennel and Wong (1967) using standard techniques. We write this result here for its appeal to generality.

The wave electromagnetic fields can always be decomposed into longitudinal components parallel to the applied magnetic field, and right and left-hand circularly rotating components in the plane normal to the applied field as follows. Suppose a given wave mode has electric and magnetic fields given

by $\underset{\sim}{E} = \underset{\sim K}{E} e^{i(\underset{\sim}{K} \cdot \underset{\sim}{x} - \omega t)}$ and $\underset{\sim}{B} (\underset{\sim}{x}, t) = \underset{\sim K}{B} e^{i(\underset{\sim}{K} \cdot \underset{\sim}{x} - \omega t)}$, where $\underset{\sim}{x}$ denotes space coordinates and t, the time. The static magnetic field B_o can be chosen to lie along the z-axis of an (x, y, z) Cartesian coordinate system. Then we can write

$$\epsilon^{\ell}_{\underset{\sim}{K}} = \left(\frac{E_x + iE_y}{\sqrt{2}}\right)_{\underset{\sim}{K}} \qquad \beta^{\ell}_{\underset{\sim}{K}} = \left(\frac{B_x + i B_y}{\sqrt{2}}\right)_{\underset{\sim}{K}}$$

$$\epsilon^{r}_{\underset{\sim}{K}} = \left(\frac{E_x - iE_y}{\sqrt{2}}\right)_{\underset{\sim}{K}} \qquad \beta^{r}_{\underset{\sim}{K}} = \left(\frac{B_x - iB_y}{\sqrt{2}}\right)_{\underset{\sim}{K}} \qquad (3.16)$$

$$\epsilon^{''}_{\underset{\sim}{K}} = E_{z, \underset{\sim}{K}} \qquad \beta^{''}_{\underset{\sim}{K}} = B_{z, \underset{\sim}{K}}$$

where ℓ and r denote left and right hand circular rotation and $''$ denotes the parallel component. It is convenient to use cylindrical coordinates in wave number $(\underset{\sim}{K})$ and velocity $(\underset{\sim}{V})$ space centered on the static magnetic field direction.

$$K_x = K_{\perp} \cos \psi \qquad V_x = V_{\perp} \cos \phi$$

$$K_y = K_{\perp} \sin \psi \psi \qquad V_y = V_{\perp} \sin \phi \qquad (3.17)$$

$$K_z = K_{''} \qquad V_z = V_{''}$$

where $_{\perp}$ and $_{''}$ denote perpendicular and parallel respectively, relative to the static magnetic field. If we assume that the growth rate $\gamma_{\underset{\sim}{K}}$ for a given $\underset{\sim}{K}$ is very small, it may be written in terms of the wave polarizations as follows:

$$\frac{\gamma_{\underset{\sim}{K}}}{|\omega_{\underset{\sim}{K}}|} = \frac{\pi}{16N} \left|\frac{\omega_{\underset{\sim}{K}}}{K_{''}}\right| \sum_{+, -} \frac{\omega^2_{p \pm}}{\omega^2} \sum_{n} \int_0^{\infty} V_{\perp}^2 dV_{\perp} \int_{-\infty}^{+\infty} dV_{''} \, \delta\left(V_{''} - \frac{\omega - n\Omega_{\pm}}{K_{''}}\right) \frac{|\theta^{\pm}_{n, \underset{\sim}{K}}|^2}{W_{\underset{\sim}{K}}} \hat{G}_{\underset{\sim}{K}} f^{\pm} \qquad (3.18)$$

where N is the equilibrium number density, $\sum_{+,-}$ denotes summation over particle species, $\sum_n$ denotes a summation of contributions from an infinite set of particle resonances, indicated by the presence of $\delta \left(\dfrac{\omega - n\Omega_{\pm}}{K_{\shortparallel}} - V_{\shortparallel} \right)$. The function $\left| \Theta_{n,\underset{\sim}{K}}^{\pm} \right|^2$ weights the strength of the wave-particle interaction at each location in velocity space, according to the polarization of the wave in question.

$$
\Theta_{n,\underset{\sim}{K}}^{\pm} = \frac{\epsilon_{\underset{\sim}{K}}^r \, e^{+i\psi} \, J_{n+1} + \epsilon_{\underset{\sim}{K}}^{\ell} \, e^{-i\psi} \, J_{n-1}}{\sqrt{2}} + \frac{V_{\shortparallel}}{V_{\perp}} \, J_n \, \epsilon_{\underset{\sim}{K}}^{\shortparallel} \tag{3.19}
$$

where J_n is a Bessel function of integral order and argument $K_{\perp} V_{\perp} / \Omega_{\pm}$. $W_{\underset{\sim}{K}}$ is the total energy, kinetic plus electromagnetic, of the wave in question, and $\widehat{G}_{\underset{\sim}{K}}$ is the following differential operator in velocity space

$$
\widehat{G}_{\underset{\sim}{K}} = \frac{K_{\shortparallel}}{\omega_{\underset{\sim}{K}}} \left\{ \left(\frac{\omega_{\underset{\sim}{K}}}{K_{\shortparallel}} - V_{\shortparallel} \right) \partial / \partial V_{\perp} + V_{\perp} \, \partial / \partial V_{\shortparallel} \right\} \tag{3.20}
$$

The $f^{\pm}$ are, of course, the equilibrium velocity distributions. $\gamma_K > 0.$ signifies instability.

When $\left| \omega / n \Omega_{\pm} \right| \ll 1$ (or equivalently $V_{\shortparallel} \gg \left| \omega_{\underset{\sim}{K}} / K_{\shortparallel} \right|$), $\widehat{G}_{\underset{\sim}{K}}$ reduces to a pitch angle gradient $-\partial / \partial \alpha$. Thus, ALL cyclotron resonances are sensitive to small pitch angle anisotropies, regardless of wave mode and angle to the field. On the other hand, the n = 0 Landau resonance depends upon $\partial f^{\pm} / \partial \left| V_{\shortparallel} \right|$ integrated over $V_{\perp}$. Landau instability arises from gradients in the $V_{\shortparallel}$ distribution. When $\partial f^{\pm} / \partial \left| V_{\shortparallel} \right| < 0$, as for plasmas without beams, currents along the lines of force, and so on, Landau resonances ordinarily contribute damping.

To obtain useful results from (3.18), it is necessary to substitute information concerning polarizations of the waves of interest into $\Theta^{\pm}_{n, \underset{\sim}{K}}$ and $W_{\underset{\sim}{K}}$. It is reasonable to use polarizations obtained from cold-plasma theory, since in first approximation the resonant particle thermal effects do not significantly change the polarizations. For the quasi-longitudinal whistler mode, we obtain thereby (Kennel, 1966)

$$\frac{\left| \Theta^{\pm}_{n, \underset{\sim}{K}} \right|^2}{W_{\underset{\sim}{K}}} = \left\{ \frac{(1 + \cos\Theta) \, J_{n+1} + (1 - \cos\Theta) \, J_{n-1}}{2\cos\Theta} \right\}^2 \tag{3.21}$$

For strictly parallel propagation, $\Theta = 0$, (3.18) and (3.21) reduce to (3.6), (3.7). Here, all the coupling strengths but one, that for the principal cyclotron resonance, vanish; $n = -1$ is unstable to mirror-type pitch angle anisotropy, as was demonstrated in section 3.2.

As Θ increases from 0, other higher cyclotron resonance particles have non-zero couplings. However, taken all together, their net effect will still be unstable for mirror pitch angle distributions (Kennel, 1966). On the other hand, the $n = 0$ Landau resonance which has zero coupling to parallel propagating electromagnetic waves will damp oblique waves. Thus the overall oblique whistler growth will be a competition between cyclotron instability and Landau damping. The cyclotron electrons are heavily weighted for small wave normal angles Θ by $\Theta^{\pm}_{-1, \underset{\sim}{K}}$; on the other hand, because the Landau electrons have considerably lower energies, roughly 100 eV, they are more numerous and should dominate at large wave normal angles, where the coupling function does not discriminate against them. The angle at which
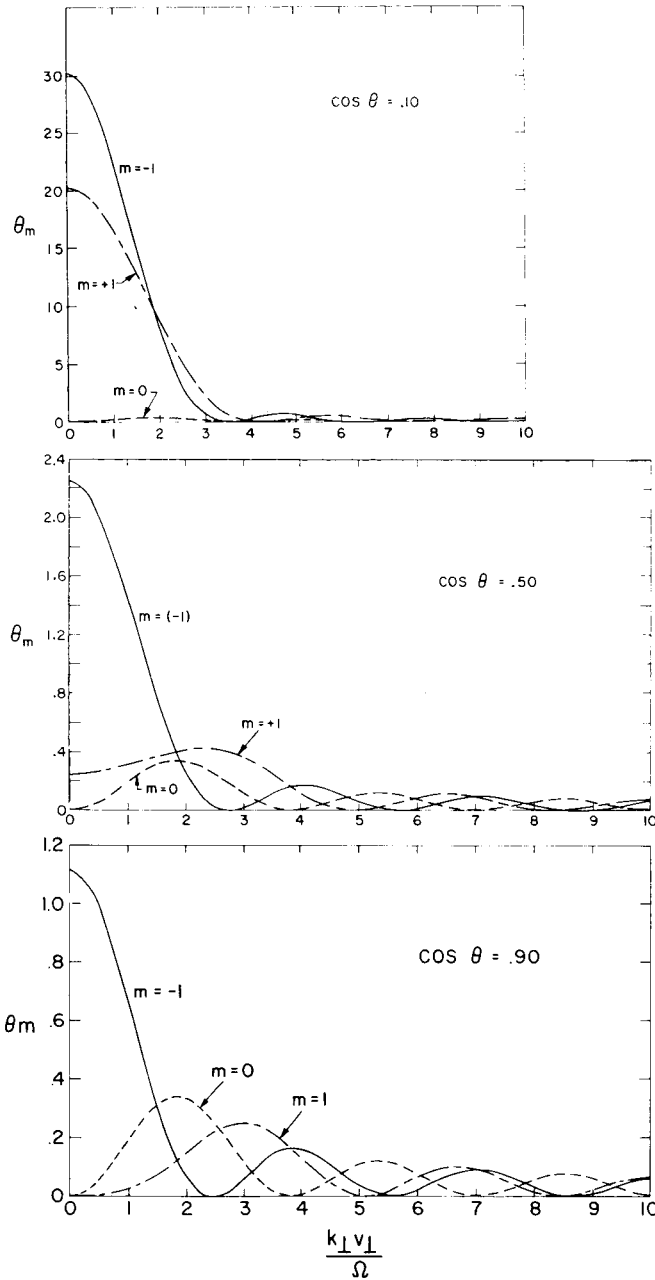
Fig. 5   Whistler-Electron Coupling Strength

$\Theta_m^{\pm}$ is plotted versus $K_\perp V_\perp / \Omega_\pm$. $\Theta_m^{\pm}$ favors the dominant $m = -1$ principal resonance quite strongly when $K_\perp V_\perp / \Omega_\pm$ is small. For large $K_\perp V_\perp / \Omega_\pm$ all resonances are weighted more or less equally. Since the velocity distribution falls off with increasing $V_\perp$, the small $K_\perp V_\perp / \Omega_\pm$ range is crucial for instability. Notice that Landau effects do not occur for $K_\perp = 0$.

-27-

A4698

Landau damping just balances cyclotron growth should depend sensitively upon the relative number of Landau and cyclotron electrons; in other words, on the energy spectrum. When the spectrum is soft there are many Landau electrons, and damping should be severe even for small Θ ; when the effective energy spectrum is hard, wave growth should occur for a large cone of propagation directions relative to the magnetic field. Numerical calculations of the whistler growth rate normalized to its value at $\Theta = 0$, are plotted in Fig. 6 as a function of Θ . To perform these calculations a pitch angle distribution corresponding to the solution of the quasi-linear diffusion given in section 4, and a power law energy dependence $1/E^p$ between Landau and cyclotron energies were chosen.

The power law energy spectrum symbolically parametrizes the relative number and velocity-space gradients of Landau and cyclotron particles. Actual distribution functions can have a more general behavior. From Fig. 6, we conclude that when the energy spectrum is sufficiently hard, effectively $\sim 1/E^2$, a large cone of wave normal angles of width $\Theta \sim 1$ radian can be unstable. When there are many more Landau electrons, i.e., a "softer" spectrum, the unstable cone shrinks rapidly. Thus the properties of the turbulent whistler spectrum depends on the number of low energy Landau electrons.

The instability calculation is somewhat more complicated for ion cyclotron waves. For mirror distributions, there is competition between damping cyclotron electrons (≈ 2 meV in the magnetosphere) damping Landau ions with ≈ 2 keV, damping Landau electrons with 2 eV and unstable cyclotron ions of ~ 100 keV (Kennel and Wong, 1966). For the outer Van Allen belts, the 2 eV Landau electrons can probably be neglected, and the ion cyclotron wave will be unstable for a large cone of wave normal angles if the effective proton energy spectrum is sufficiently hard, again roughly $1/E^2$.
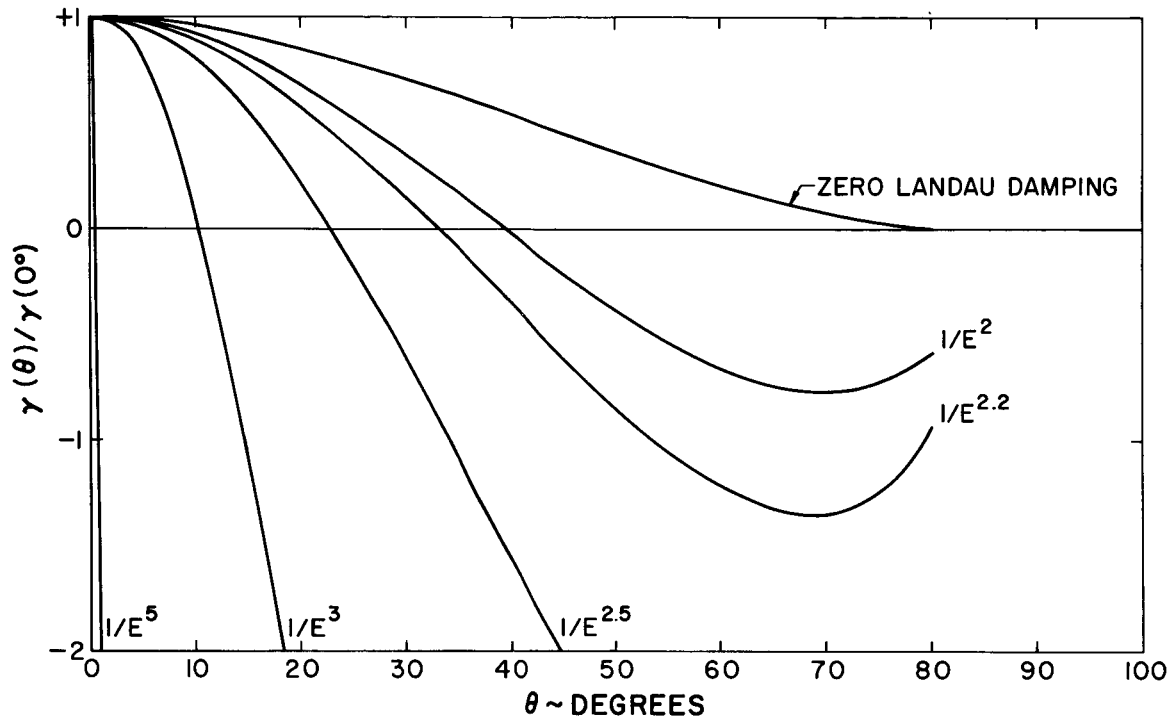
Fig. 6   Whistler Growth Rate

Plotted here is $\gamma(\Theta)/\gamma(0^\circ)$, the ratio of the obliquely to parallel propagating whistler growth rates, as a function of the strength of Landau dumping, for a mirror electron distribution. Here we have plotted the sum of the $n = \pm 1$ and $n = 0$ electron partial growth rates. Higher cyclotron electron resonances $|n| > 1$ will make the system slightly more unstable than shown in the diagram while the protons will damp the waves very slightly. When Landau damping is neglected, whistlers are unstable at all propagation angles. The precise width in Θ of the unstable spectrum is very sensitive to the relative number of Landau and cyclotron electrons, parametrized here by power law electron energy spectra.

-29-

3.5)   Instability along Realistic Whistler Trajectories

3.5a)   Calculation of Local Increment of Growth

Now we are in a position to combine the growth rates for obliquely propagating whistlers computed in section 3.4 with the ray path calculations of section 3.3. To investigate the competition between cyclotron growth as a given whistler propagates along the field through the equatorial plane and Landau damping on the high latitude portion of its ray path where its wave normal is nearly perpendicular to the magnetic field, we plot in Fig. 7 the local increment of growth as a function of geomagnetic latitude along the ray path. We have selected as an example a wave initially propagating parallel to the magnetic field in the equatorial plane. We have normalized the growth rate up the line of force, $\gamma(\lambda)$, to its value at $\lambda = 0$. Thus, we cannot learn from these plots the magnitude of the net growth rate -- this depends at any rate on the number of trapped cyclotron electrons -- but we can tell whether or not the whistler will be unstable overall.

The resonant electrons are parametrized by an inverse power law $1/E^p$ energy spectrum between Landau and cyclotron energies, and have pitch angle distribution consistent with the solution of a steady state quasi-linear pitch angle diffusion equation, for reasons to be discussed in section 4. A hard $p = 2$ effective electron energy spectrum permits a thin region of width $\Delta\lambda \sim 20^\circ$ about the equatorial plane of growth for the whistler mode. The softer $p = 3$ electron energy spectrum is heavily Landau damped over most of the ray path, while $p \approx 2.5$ is marginally stable.
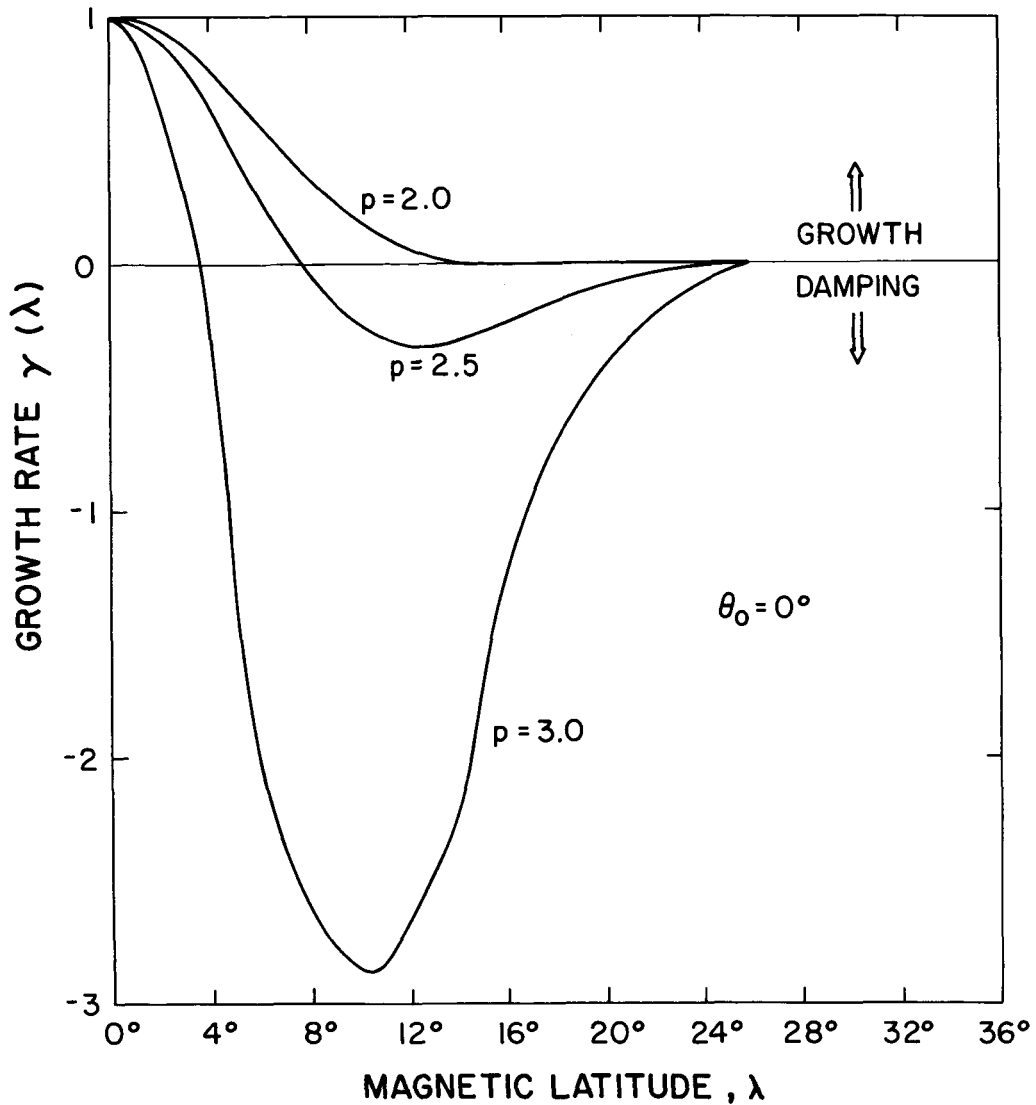
Fig. 7   Local Increment of Whistler Growth

This figure combines the results of Fig. 6 with the ray
path calculations of Fig. 5. Here we plot $\gamma(\lambda)$, the
local increment of growth at the geomagnetic latitude λ,
for a wave initially propagating parallel to the lines of
force at the equator. p is the index of the energy spectrum.
Landau damping confines the region of growth to quite near
the equatorial plane. At latitudes $\lambda \geq 20°$, there are very
few resonant particles and there is at best a small change
in the wave amplitude beyond this point. The p > 2.5 electron
energy spectrum is approximately marginally stable,
integrated over the ray path.

For different choices of total density distributions N along the lines of force, the wave normal angles will rotate to large angles more or less slowly with latitude then for these calculations. If they do so more slowly, the waves may not reach damping wave normal angles except at high latitudes, where even the number of Landau electrons is small. In this case, Landau damping effects will be less pronounced.

3. 5b) Estimate of Number of Landau Electrons

Figure 8 is a schematic idealized summary of our knowledge of the electron energy distribution for a mixed auroral-Van Allen line of force. This has significant trapped fluxes of both auroral (1-10 keV) and Van Allen (40 keV) electrons, and is a somewhat special choice, since Gurnett and Fritz (1965), O'Brien (1966) and others have noticed that usually one type of particle is found without the other. However, the "overlap" lines of force, with the mixed electron population, are the most active geophysically. We therefore devote our attention to this case. Since most electron detectors have energy thresholds, it is convenient to plot $n(>E)$, the number density of electrons with energies greater than E , as a function of energy.

Serbu and Maier (1966) have measured a total electron density of roughly 30 cm^3. Estimates from observations of the dispersion of whistler waves (Carpenter, 1966) and hydromagnetic waves (Watanabe, 1965) suggest electron densities perhaps an order of magnitude smaller. We plot both measurements as an indication of the uncertainty in our knowledge of the present time. Measurements of auroral electrons
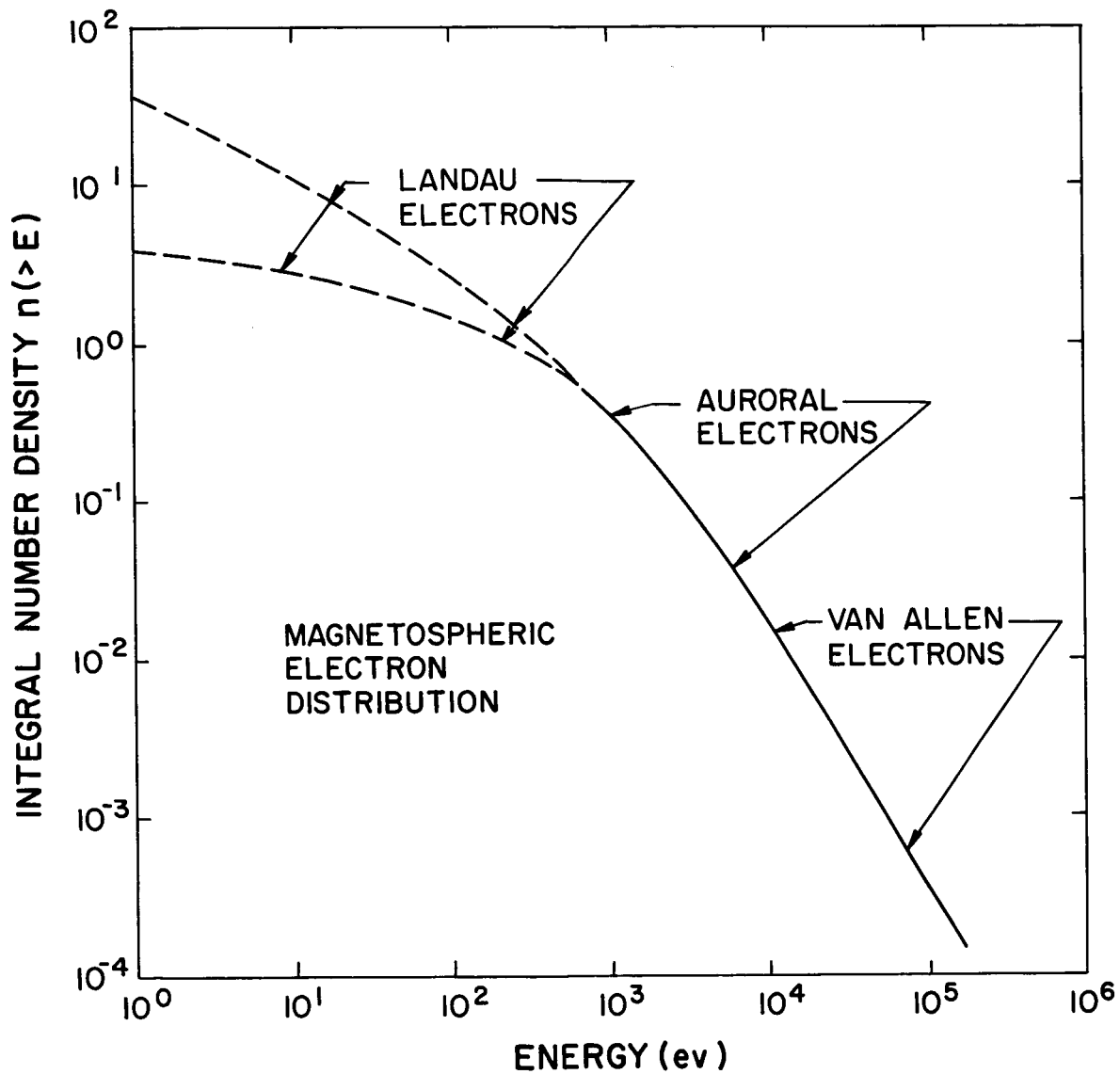
Fig. 8   Electron Distribution in the Magnetosphere

This figure is meant to leave an impression of the locations
in the velocity distribution of the various groups of electrons
discussed in the text and a rough guess as to their fractional
density.

suggest fluxes of roughly 10^9 cm^2-sec (see Ness, 1965, for a review of these measurements) which suggest electron densities of roughly 0.5 cm^3. Finally electrons >40 keV have fluxes of 2 x 10^7 cm^2-sec, (Frank, 1965) implying $n(>40 \text{ keV}) \approx 2 \times 10^{-3}/cm^3$; above 40 keV the fluxes and number densities appear to fall off roughly as $1/E^2$ (McDiarmid and Burrows, 1964).

Unfortunately, the experimental information directly concerning the electrons most likely to be responsible for whistler damping, hundred electron volt Landau electrons, is quite sparse. The higher energy cyclotron electrons do have a $1/E^2$ energy spectrum above 40 keV and on the basis of the present evidence, it seems reasonable that the energy spectrum between 40 keV and 100 eV be no softer than $1/E^2$.

On the basis of the present admittedly sparse evidence, Landau electrons do not appear to be sufficiently intense to appreciably suppress whistler growth. They should however define the width in Θ of the unstable wave distribution in the equatorial plane. When the Landau fluxes are intense, whistler instability could well be suppressed. In this case, the regions of wave growth shrink while those of damping increase in size. However, in the equatorial plane where the growth rates are locally positive, there could still be a large fluctuation levels of whistlers which build up from the thermal background even when the whistlers are not unstable overall.

3.5c)   Ion Cyclotron Wave Discussion

Without accurate ray path calculations for unducted ion cyclotron waves, it is difficult to draw exact conclusions as to their overall instability. However, it is intuitively clear that ion cyclotron waves will

tend, as they propagate, to rotate their wave vector thereby enhancing Landau damping. Nevertheless, when the proton energy spectrum between 1-100 keV is sufficiently hard, effectively $\sim 1/E^2$, a large cone of wave normal angles can be unstable, (Kennel and Wong, 1966) thereby probably insuring overall instability along the ray paths. A significant complication in the case of ion cyclotron waves is the fact that cold electrons can Landau damp these waves. These may be important in the inner magnetosphere $L \sim 3\text{-}4$, where the ionosphere can be an appreciable source of cold electrons.

3.5d) Summary

From the arguments of the previous sections, we conclude that whistlers and ion cyclotron waves are unstable when the high energy cyclotron particles in the electron and ion distributions, respectively, are sufficiently intense, possess a mirror pitch angle anisotropy, and the corresponding Landau particles are not too intense. The region of growth can be narrow and confined to the equatorial plane by Landau damping. Neither growth nor damping is significant at latitudes $\lambda \gtrsim 20^\circ$ because the resonant particle energies become extremely large at high latitudes.

3.6) Criterion for Instability

In the previous sections we discussed the conditions necessary for the wave growth rates due to resonant particle interactions to have a positive sign. These considerations essentially placed limitations on the pitch angle distributions of cyclotron particles, and the relative Landau-cyclotron particle intensities, but did not restrict the number

of cyclotron particles. Since in all realistic configurations there are mechanisms of wave energy loss which do not involve resonant particles, there must also be a critical cyclotron particle intensity for instability, in order to overcome non-resonant losses.

We estimate the onset particle intensity using a schematic model to estimate the losses of wave energy. As each whistler and ion cyclotron wave crosses the equatorial plane, it increases its amplitude. If it then propagates out of the system without encountering another region of gain, the wave energy would be lost directly. The process of amplification can be greatly aided if the waves could reflect a few times back and forth across the equatorial plane. We call this the laser model of wave growth.

Such reflection mechanisms are bound to exist. Kimura (1966) and Thorne and Kennel (1966) suggested that a process similar to a complete internal reflection takes place at the lower hybrid resonance for those whistlers which propagate nearly normal to the magnetic field. From the arguments of section 3.3, most whistlers will encounter the LHR at magnetic latitude of 45 degrees or less, well away from the Earth's surface. This leads to the idea of a magnetospheric cavity in which both waves and particles are quasi-trapped and bounce back and forth across the equatorial plane. Whistlers tend to walk outwards, and after four or five bounces probably leave the magnetosphere.

Another reflection mechanism has been proposed by Stix (1964). In the presence of a density gradient, whistlers travelling away from the equator are converted at the LHR to ion acoustic waves which then are ·reflected back towards the equatorial plane. The ion acoustic waves could

then be reconverted to whistlers at the LHR in the opposite hemisphere. Finally, Berk, Horton, Rosenbluth, and Sudan (1966), have pointed out that if one treats reflection not by the geometrical optics WKB approximation but by the more accurate Bremmer method, a reflected wave always exists when the medium is inhomogenous. No special mechanisms are needed. Although the reflected return is exponentially small (and therefore not found in the geometrical optics approximation), it can be significant for inhomogeneous media with gain where the waves can grow exponentially rapidly.

Whether or not the reflection model is reasonable in all cases, we can lump all our ignorance about the manifold non-resonant reflection and wave loss processes in the magnetosphere into an effective reflection coefficient. Then the criterion for overall instability is that resonant-particle growth overcome all other wave energy losses. If $d\ell$ is an element of ray path, and V_G the group velocity, the instability criterion is

$$e^{\int_{\ell_1}^{\ell_2} \frac{\gamma(\ell)d\ell}{V_G}} \geq 1/R \qquad (3.22)$$

where R is the effective reflection coefficient, and ℓ_1 and ℓ_2 are the wave reflection points.

(3.22) is much too complex to permit a comparison with observations. Since γ is largest and V_G smallest in the equatorial plane, the growth rate integral is dominated by the contributions from the equatorial plane, γ_o, V_{Go}. Therefore, (3.22) reduces crudely to

$$\gamma_o > \frac{V_{Go}}{L} \ln 1/R \qquad (3.23)$$

where L , the effective length of the growth region, should depend somewhat on the energy spectra of the trapped Landau and cyclotron particles. Usually it is convenient to use γ_o for the parallel waves, $\Theta = 0$, in (3.23). Note that (3.23) is relatively insensitive to the reflection mechanisms because of the logarithmic dependence upon R .

Because the magnetosphere is a highly variable environment, we have not attempted to derive an accurate stability criterion for whistlers and ion cyclotron waves, but have simply outlined in intuitive terms some of the factors which determine stability. The most important of these is the intensity and pitch angle distribution of high energy cyclotron particles. These determine the stability of parallel propagating waves. Next comes the rate at which the wave normal angle is rotated as the wave propagate. This depends upon the spatial distribution of N and B . Finally, the distribution of lower energy Landau particles helps determine the damping rate of obliquely propagating waves, the thickness of the region of gain near the equatorial plane, and the spread of wave-normal angles in the turbulent spectrum. In a system depending upon so many interrelated parameters, many different complex phenomena will probably be observed at different times.

4. General Properties of Weak Electromagnetic Wave Turbulence

4.1) General Diffusion Rate

Having established a reasonable case for the growth of whistlers and ion cyclotron waves in the magnetosphere, we investigate some of the non-linear consequences of such growth. To second order in the wave amplitude, two such consequences may be identified: quasi-linear diffusion of particles in velocity space (Drummond and Pines, 1962; Vedenov, et al, 1962) and non-linear coupling of wave modes (Fishman, et al, 1960; Camac, et al, 1962; Drummond and Pines, 1962). For the above wave modes in the magnetosphere, velocity space diffusion turns out to be the more important effect.

Velocity space diffusion has been discussed by many authors. A simple expression for the diffusion equation for waves of any oscillation branch propagating at an arbitrary angle to the magnetic field has been derived by Kennel and Engelmann (1966). We reproduce this here because it is closely related to the general growth rate formula, Eq. (3.18), given previously.

$$\frac{\partial f^{\pm}}{\partial t} = \lim_{V \to \infty} \sum_{n} \frac{\pi e^2}{M_{\pm}^2} \int \frac{d^3K}{(2\pi)^3 V} \left\{ \left[\widehat{G}_{\underset{\sim}{K}} + \left(1 - \frac{K_{\parallel} V_{\parallel}}{\omega_{\underset{\sim}{K}}} \frac{1}{V_{\perp}} \right) \right] \left[\left| \Theta^{\pm}_{n,\underset{\sim}{K}} \right|^2 \delta(\omega_{\underset{\sim}{K}} - K_{\parallel} V_{\parallel} - n\Omega_{\pm}) \right] \widehat{G}_{\underset{\sim}{K}} \right\} f^{\pm}$$

$$(4.1)$$

V is the volume of the plasma, considered to be very large, $\int d^3K$ denotes an integration over all waves in the turbulent spectrum, $\widehat{G}_{\underset{\sim}{K}}$ is the velocity space operator defined in (3.20), $\Theta^{\pm}_{n,\underset{\sim}{K}}$ is defined by (3.19), and the delta function once again limits the diffusion to that due to resonant wave-particle interactions.

4.2) Pitch Angle Diffusion

Since for $V_{\parallel} \gg \omega/K_{\parallel}$ or equivalently $\omega/n\Omega_{\pm} \ll 1$, the operator $\widehat{G}_{\underset{\sim}{K}}$ reduces to a pitch-angle gradient, the diffusion at all cyclotron harmonics is primarily in pitch angle at all cyclotron harmonics. The energy diffusion rate is $0\,(\omega^2/n^2\Omega_{\pm}^2)$ smaller than the pitch angle diffusion rate. The fact that the precipitation observations cited in section 2 require changes in pitch angle without much change in energy suggests that cyclotron resonance quasi-linear diffusion must be responsible for the observed precipitation.

Rather than solve the quasi-linear Eq. (4.1) in all its complexity, we simplify it by assuming that cyclotron diffusion is purely in pitch angle, and that the wave spectrum in K-space is smooth and broadband. Then (4.1) reduces to the form derived by Kennel and Petschek (1966)

$$\frac{\partial f^{\pm}}{\partial t} = \frac{1}{\sin\alpha}\,\partial/\partial\alpha\,(D^{\pm}\sin\alpha\,\partial f^{\pm}/\partial\alpha) \qquad (4.2)$$

where $\alpha = \tan^{-1} V_{\perp}/V_{\parallel}$, the pitch angle, and $D^{\pm}$, the diffusion coefficient, is roughly

$$D^{-} \approx \Omega_{-}\,\beta_{\omega}/|\cos\alpha| \;;\; \text{whistlers}$$

$$\qquad\qquad\qquad (4.3)$$

$$D^{+} \approx \Omega_{+}\,\beta_{\omega}/|\cos\alpha| ;\; \text{ion cyclotron waves}$$

where $\beta_{\omega} = (B)^2/B_{o}^2$, the wave beta, is the ratio of total wave magnetic energy in the appropriate mode to static magnetic energy. $1/D^{\pm}$ is roughly the time a particle takes to random walk a radian in pitch angle.

4.3) Landau Diffusion

By setting $V_{\parallel} = \omega/K_{\parallel}$ in the velocity space gradient $\widehat{G}_{\underset{\sim}{K}}$, we see that diffusion at the Landau resonance scatters particles in $V_{\parallel}$ without

changing $V_\perp$. For electromagnetic waves, the coupling function $\theta^\pm_{0, \underset{\sim}{K}}$ is

zero when $K_\perp = 0$. Thus, Landau diffusion only occurs in a wave spectrum

which includes obliquely propagating waves. $n = 0$ Landau diffusion cannot

account for the precipitation observations for two reasons. First of all,

since $V_\perp$ does not change, Landau particles can only reach the loss cone by

increasing their parallel, and therefore, total energy. This contradicts

the observations of precipitation without significant energization. Secondly,

the wave-particle coupling for $V_\perp \approx 0$ Landau particles tends to be rather

small. Thus once particles reach the neighborhood of the loss cone, it takes

a long time for them to diffuse into it.

We have argued previously that low energy Landau particles can, in

certain cases, determine the stability properties of the whistler and ion

cyclotron waves. We will show in section 5 that pitch angle diffusion sets

the pitch angle distribution of cyclotron particles. However, because the

Landau energies differ greatly from cyclotron energies, and because Landau

diffusion is not pitch angle diffusion, the properties of the Landau particles

in the magnetosphere will be determined by essentially independent

diffusion properties and distributions of sinks and sources.

4. 4)   Non-linear Wave-Wave Couplings

Non-linear mode couplings can affect the magnetospheric diffusion

problem in at least two ways. First, the wave spectrum could change due

to mode-mode couplings on time scales short compared with the particle

diffusion time, $1/D^\pm$. This is not the case for whistlers. Camac, et al

(1962), Karpman and Galeev (1963) and others have calculated the mean

"collision frequency" ν between two whistlers interacting non-linearly.

.This is roughly

$$\nu \approx \omega\beta_\omega \qquad (4.4)$$

Thus, when $\omega/\Omega_- \ll 1$, as for Van Allen electrons, the whistler spectrum is essentially constant during the time the cyclotron electrons diffuse into the loss cone.

The frequency of ion cyclotron waves decreases with increasing wave number, unlike that of the low frequency whistlers. For this reason, resonant three-wave mode couplings of the whistler type are forbidden, since energy and momentum cannot both be conserved in the mode interaction (Camac, et al, 1962; Galeev and Karpman, 1963). Therefore, the lowest order ion cyclotron wave coupling is the four-wave interaction, which depends on the square of the wave beta.

$$\nu \approx \omega\beta_\omega^2 \qquad (4.5)$$

In addition, in the $\omega \to 0$, $K \to 0$ limit, the ion cyclotron mode reduces to the familiar torsional Alfven wave, which is always linear (Kantrowitz and Petschek, 1964). In this limit, all mode couplings are zero. For both these reasons, we expect ion cyclotron mode couplings with each other to be small.

Another condition which must be satisfied is that the mode-coupling rate be much smaller than the wave growth (or escape) rate. If this is so, the non-linear growth of wave amplitude will saturate by velocity space plateau formation and not by mode-coupling. For the magnetosphere the growth rates will be given roughly by (3.23) and so we require for whistlers

$$\frac{\nu}{\gamma} \approx \frac{\omega\beta_\omega}{\frac{V_{Go}}{L}\ln 1/R} \ll 1 \qquad (4.6)$$

β_ω in the equatorial plane may be estimated from the observed precipitation lifetimes using Eq. (4.3). Condition (4.6) is satisfied throughout the Van Allen zone, though perhaps not in the auroral zone where the precipitation rates are quite high.

5. Upper Limit to Stably Trapped Particle Fluxes

5.1) Theoretical Estimate

The stability criteria discussed in section 3 clearly restrict the energetic particle distributions which can be stably trapped in the magneto-sphere. However, considerable freedom still remains since the growth rate depends in general upon the intensity of trapped particles and their distribution in energy and pitch angle. A very intense but nearly isotropic trapped particle flux could well be stable while a weak, highly anisotropic flux might be unstable. However, the experimental observation that acceleration sources of new particles exist can further restrict the class of stable distribution functions. In this case, acceleration will increase the trapped cyclotron particle flux until instability occurs, regardless of the initial pitch angle anisotropy. As the unstable waves grow, quasi-linear pitch angle diffusion inevitably occurs, and the pitch angle distribution is then fixed by the distribution of sources and sinks in velocity space, and all information about initial anisotropies is lost. In other words, we ask what is a "reasonable" pitch angle anisotropy to insert in the instability criterion, (3.23)? This should be consistent with the existence of turbulence and the sources and sinks of resonant particles which ultimately drive the turbulence. Once the anisotropy is fixed by diffusion arguments, Eq. (3.23) leads to an estimate for the upper limit to stably

trapped cyclotron particle intensities. Furthermore, since an unstable wave distribution diffuses cyclotron particles into the loss cone, the observed cyclotron particle flux intensities should not exceed the critical intensity for instability.

The instability analysis of section 3 clearly indicates that the growth for unducted whistlers is largest in a narrow latitude region in the equatorial plane. Since Landau damping sets in at higher latitudes, the wave intensities, and therefore diffusion coefficients, should be largest near the equatorial plane. Each time an electron crosses the equatorial plane it has a reasonable probability of a cyclotron resonance interaction with the whistler distribution there; however, at higher latitudes, its motion will be essentially adiabatic, as it will be out of cyclotron resonance with the waves at high latitudes, whose amplitudes in any case will be at least somewhat smaller than in the equatorial plane. Since the pitch angle diffusion region is thin, it is appropriate to treat it as uniform. We will consider the idealized problem of pitch angle diffusion in an infinite homogeneous plasma. The precipitation lifetimes so obtained will be some fraction of the actual lifetimes, since the actual electrons spend only a fraction of each bounce period in the diffusion region. It is clear that we are allowed to consider with this model only diffusion processes which have characteristic time scales much longer than the particle bounce period, roughly one second for electrons.

To estimate the pitch angle anisotropies which could be encountered in the turbulent magnetosphere, Kennel and Petschek (1966) considered an idealized steady state where particle diffuse in pitch angle from a source S at flat pitches

$$S(E,\alpha) = S(E)\delta(\alpha - \pi/2) \tag{5.1}$$

into the loss cone at small pitches, $\alpha = \alpha_0 \ll 1$.

We estimate this atmospheric loss rate by

$$L(E, \alpha) = f(E, \alpha) \frac{V_{\shortparallel}}{\ell} : \begin{array}{l} 0 \leqslant \alpha \leqslant \alpha_o \\ \pi - \alpha_o \leqslant \alpha \leqslant \pi \end{array}$$

$$= 0, \quad \alpha_o \leqslant \alpha \leqslant \pi - \alpha_o \tag{5.2}$$

ℓ is the distance along a line of force from the diffusion region in the equatorial plane to the atmospheric scattering point. In other words, once particles reach the loss cone, they leave the diffusion region by freely travelling along the line of force. Naturally, we must average over many particle bounce periods between mirror points in this model.

Since cyclotron particles diffuse in pitch angle alone, their energy distribution is fixed by the acceleration mechanism, and by the dependence of the critically unstable flux upon energy. Assuming that the diffusion rate is sufficiently slow relative to the bounce period, the number of particles at the edge of the loss cone is small, and the diffusion equation (4.2) then has the following simple solution with the sink (5.2) and source, (5.1):

$$f(E,\alpha) = \begin{cases} \doteq 0 \quad 0 \leqslant \alpha \leqslant \alpha_o, \ \pi - \alpha_o \leqslant \alpha \leqslant \pi \\ \\ = \dfrac{S(E)}{D} \begin{cases} \log \dfrac{\sin \alpha}{\sin \alpha_o} \quad : \dfrac{\pi}{2} \geqslant \alpha \geqslant \alpha_o \\ \\ \log \dfrac{\sin(\pi-\alpha)}{\sin(\pi-\alpha_o)} : \dfrac{\pi}{2} \leqslant \alpha \leqslant \pi - \alpha_o \end{cases} \end{cases} \tag{5.3}$$

This regime, the one normally encountered in the Van Allen Belts, we call "weak" diffusion.

When the diffusion rate is so rapid, owing to an exceptionally strong source, that particles can random walk in pitch angle across the loss cone in less than a bounce period, the loss term can be neglected. In this limit,

the steady pitch angle distribution is isotropic. The maximum allowable precipitation rate corresponds to removing all the particles in the now isotropic distribution at their free velocity along the lines of force. This corresponds to a minimum lifetime T^* which depends only upon the size of the loss cone and not upon the pitch angle diffusion rate.

$$T^* \sim \frac{2\ell}{V_{||} a_o^2} \tag{5.4}$$

This strong diffusion limit, mentioned for completeness, is probably important only for the intense precipitation in the auroral zone and not in the Van Allen Zone, where the precipitation rates are smaller.

Thus, for turbulent pitch angle distributions, there is a marginally stable partial density η_-^* of electrons in cyclotron resonance, given by inserting (5.3) into (3.23) for whistlers:

$$\eta_-^* \approx \frac{V_{A-}}{\Omega_- L} \ln 1/R \tag{5.5}$$

$V_{A-} = \dfrac{B_o}{(4\pi N M_-)^{1/2}}$ is the electron Alfven velocity, and we have suppressed constants of $0(1)$ in (5.5). V_{A-}/Ω_- is the electron gyroradius based on the electron Alfven speed. If the unstable region is many gyroradii long, $L \gg V_{A-}/\Omega_-$, η_-^* does not need to be large to ensure instability.

Similar reasoning leads to the upper limit for stably trapped protons

$$\eta_+^* \sim \frac{V_{A+}}{\Omega_+ L} \left(\frac{\omega}{\Omega_+}\right) \ln 1/R \tag{5.6}$$

Noting that for the resonant ions of energy E, $\dfrac{8\pi N E}{B_o^2} \sim \left(\dfrac{\Omega_+}{\omega}\right)^2$ we can convert formula (5.6) into that derived by Cornwall (1966):

$$\frac{(\eta_+^* N) E}{B^2/8\pi} \sim \frac{V_{A+}}{L\omega} \ln 1/R \tag{5.7}$$
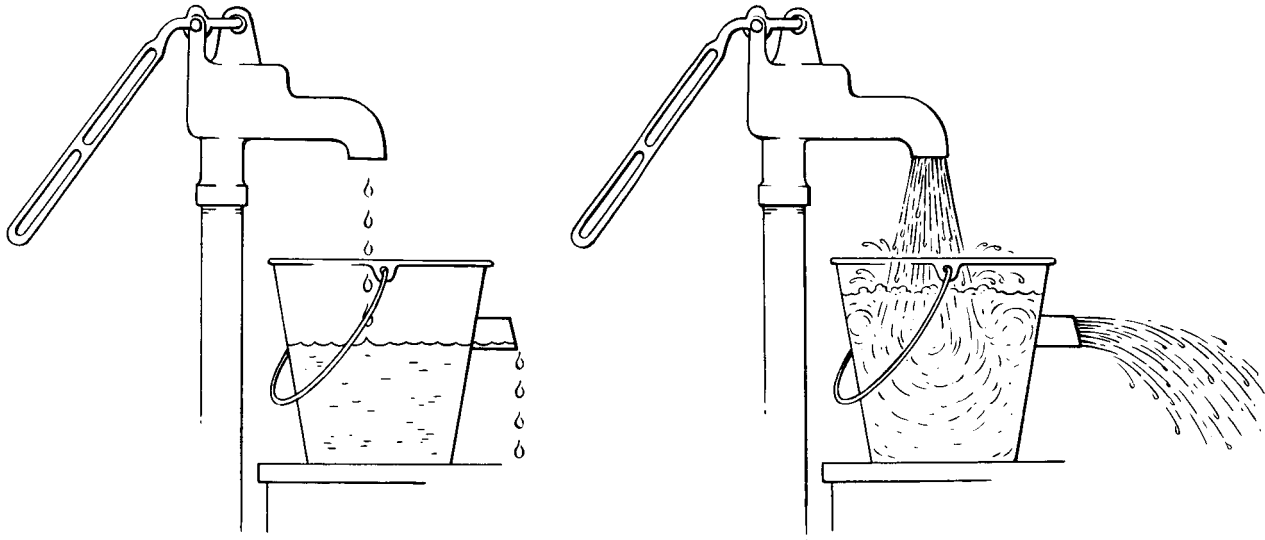
WEAK DIFFUSION
40 KeV ELECTRONS

STRONG DIFFUSION
AURORAL ELECTRONS (5 KeV)

Fig. 9   Weak and Strong Diffusion

Visualized here, in terms of the "Leaky Bucket" analogy
of O'Brien (1964 and 1966), is the difference between weak
and strong diffusion. Since whistler and ion cyclotron
turbulence can at best create pitch angle isotropy and the
loss cone has a finite size, there is a maximum precipitation
rate. When the source of new particles is weak, the fluxes
are limited by losses. However, a strong source can fill
up the loss cone, and particles will again accumulate.
This may occur in the highly turbulent auroral zone.

Just as for whistlers when there are many Alfven ion gyroradii in the unstable region, instability can occur for a low fractional density of energetic cyclotron resonance ions.

It should be noted that we have, for simplicity, tacitly employed the laser model for precipitation. This requires a hard energy spectrum for weak Landau damping and therefore long unstable ray paths, and reflection points such as, for instance, those at the lower hybrid resonance. This model probably establishes the lowest critical particle fluxes. However, when the spectrum is soft, the unstable region shrinks. Nevertheless, significant precipitation can still take place even if the waves are not unstable overall. All that is needed is a sufficiently large enhancement of the thermal fluctuation wave intensity near the equatorial plane. This may be achieved by allowing the trapped cyclotron particle fluxes to build up to a sufficiently high level, somewhat above the previously calculated onset fluxes. Since waves grow exponentially, orders of magnitude flux enhancements are not needed. Thus, flux limitation is bound to occur at some point.

Cornwall (1966) has suggested that when the source of accelerated protons is sufficiently large, ion cyclotron driven precipitation may become unsteady. The concept of nonsteady precipitation is contained in the afore-mentioned maximum allowable precipitation rate. A source which adds particles faster than they can be removed by precipitation clearly leads to nonsteady behavior. Future research in this direction may help explain the fascinating variety of unsteady wave emission and particle loss processes observed in the magnetosphere.

5.2) Comparison with observations

5.2a) Trapped Electrons

At the high energy end of the electron spectrum, where $|\omega/\Omega_-| \ll 1$ for all cyclotron resonant whistlers, the limiting flux is only a weak function of electron energy. Thus, cyclotron electrons of lower energy are more likely than those of very high energy to be near the critical flux for whistler instability, since there are more of them. The limiting flux is a strong function of location in space, since it depends on the length of the unstable region (in turn dependent upon Landau electrons), and upon the group velocity and local electron gyrofrequency. In Fig.10 we have plotted the limiting fluxes for cyclotron electrons >40 keV, using estimates for the equatorial plane magnetic field strength and number density for the noon, dawn and evening and midnight meridians, as a function of radial distance from the center of the Earth. Superimposed on these estimates is the range, minimum to maximum, of electron fluxes >40 keV, observed near the equatorial plane over a ten-month period by Explorer XIV (Frank, 1965) and also the average precipitated fluxes observed by Injun III (O'Brien, 1964) near the Earth. At distances greater than three or four earth radii, the trapped fluxes were at times sufficiently intense to cause whistler instability, and precipitation tended to occur in agreement with theory. Closer to the Earth, the calculated limiting electron flux is very large, and the observed precipitation is less intense. Higher energy electrons appear less often to be near their limiting flux (Kennel and Petschek, 1966) and consequently do not precipitate as intensely (O'Brien, 1964).
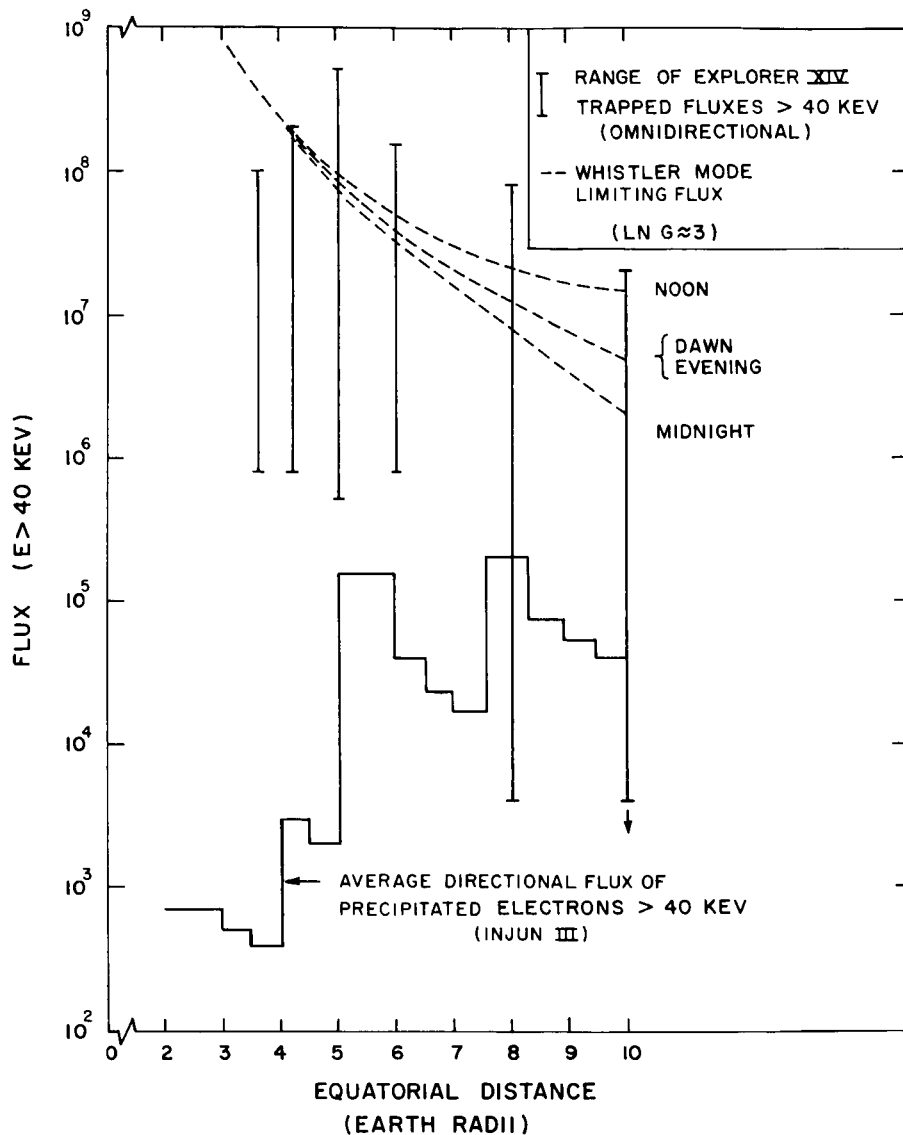
Fig. 10   Limitation on trapped > 40 keV electron fluxes. The
theoretical limiting flux J* is compared with Explorer 14
equatorial trapped fluxes as a function of the equatorial
radial distance. The largest observed trapped fluxes are
indeed close to the theoretical upper limit. We also show
the distribution with L shell of Injun 3 precipitated electrons.
As expected, strong precipitation occurs only where trapped
fiuxes can be comparable with the calculated limiting flux.
The distributions of precipitated and trapped electrons
> 40 keV appear to be mutually consistent.

-50-

Figure 11 permits an estimate of the long term behavior of the Van Allen Belt >40 keV cyclotron electrons. Plotted are Explorer XIV fluxes measured near the equatorial plane over a ten-month period. The observed electron intensities were more often subcritical than unstable. Furthermore, the whistler mode upper limit appears to be a good one, in the sense that the trapped fluxes are often near their critical intensity limit. This suggests that all other instabilities which could also limit the Van Allen electron flux have higher onset trapped electron intensities.

5.2b)   Trapped Proton Fluxes

Figure 12 compares the trapped ion fluxes measured by Explorer XII (Davis and Williamson, 1963) with the ion cyclotron upper limit to the proton fluxes. Again the agreement is reasonable. An interesting feature is that the trapped ion critical fractional number densities can be a factor 40 larger than the corresponding limiting number densities for electrons. Thus, most of the high energy particles in the magnetosphere are protons, when acceleration keeps both electron and proton fluxes near the onset intensity for instability. Cornwall (1966) has also discussed the trapped proton fluxes and found reasonable agreement with the criterion (5.7).

5.2c)   Whistler Wave Intensity

The observed Van Allen electron lifetimes correspond to wide-band whistler magnetic field amplitudes in the equatorial plane of 10^{-2}-10^{-3} γ, where $1\gamma = 10^{-5}$ gauss (Kennel and Petschek, 1966). As we have indicated, the region of very large wave amplitudes could be localized to the equatorial plane, since there the growth is positive and Landau damping and other wave losses limit the amplitude away from the equatorial plane. In addition,

10^9

J_o 10^7 10^5

• $0° \leq \lambda \leq 15°$
○ $15° \leq \lambda \leq 30°$

THEORETICAL LIMIT

L=5

J_o 10^8 10^6 10^4

L=6

J_o 10^7 10^5 10^3

THEORETICAL LIMIT

L=8

J_o 10^6 10^4

L=10

| 7 14 21 | 1 7 14 21 | 1 7 14 21 | 1 7 14 21 | 1 7 14 21 | 1 7 14 21 | 1 7 14 21 | 1 7 14 21 | 1 7 14 21 | 1 7 14 21 28 |
OCT | NOV. 1962 | DEC. | JAN. | FEB. | MAR | APR. 1963 | MAY | JUNE | JULY
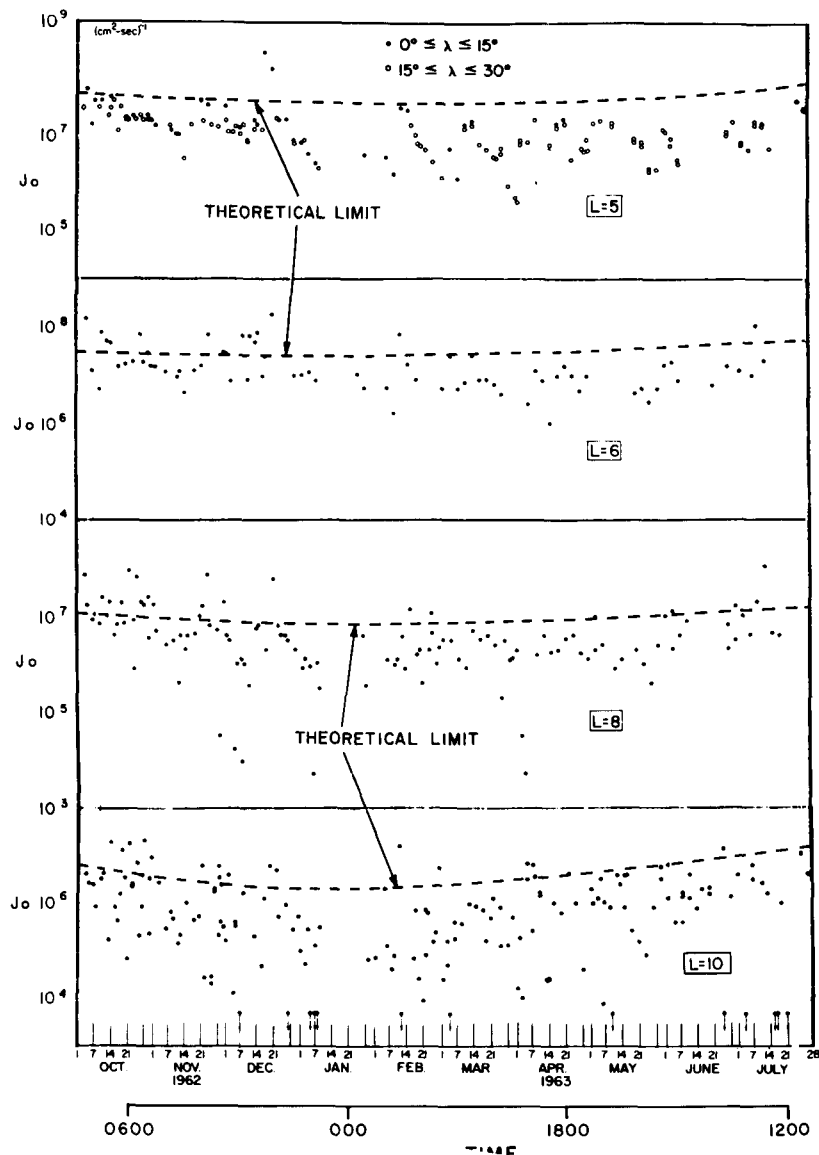
0600   000   1800   1200

TIME

Fig. 11   Limitation on trapped electrons > 40 keV. This diagram permits an estimate of the degree to which observed particle fluxes approach their limiting value. We have superposed the calculated J* on Explorer 14 data published by Frank (1965). The majority of points are clearly below the predicted limit. The small scatter of points near but below the limit at L = 6 suggests that a continuous acceleration mechanism is operative here. The electron fluxes > 40 keV seem nearest their precipitation limit on the morning side of the Earth, where precipitation is known to be high. The large scatter of points at L = 10 may arise from the other violent processes which are expected to occur in the auroral zone.
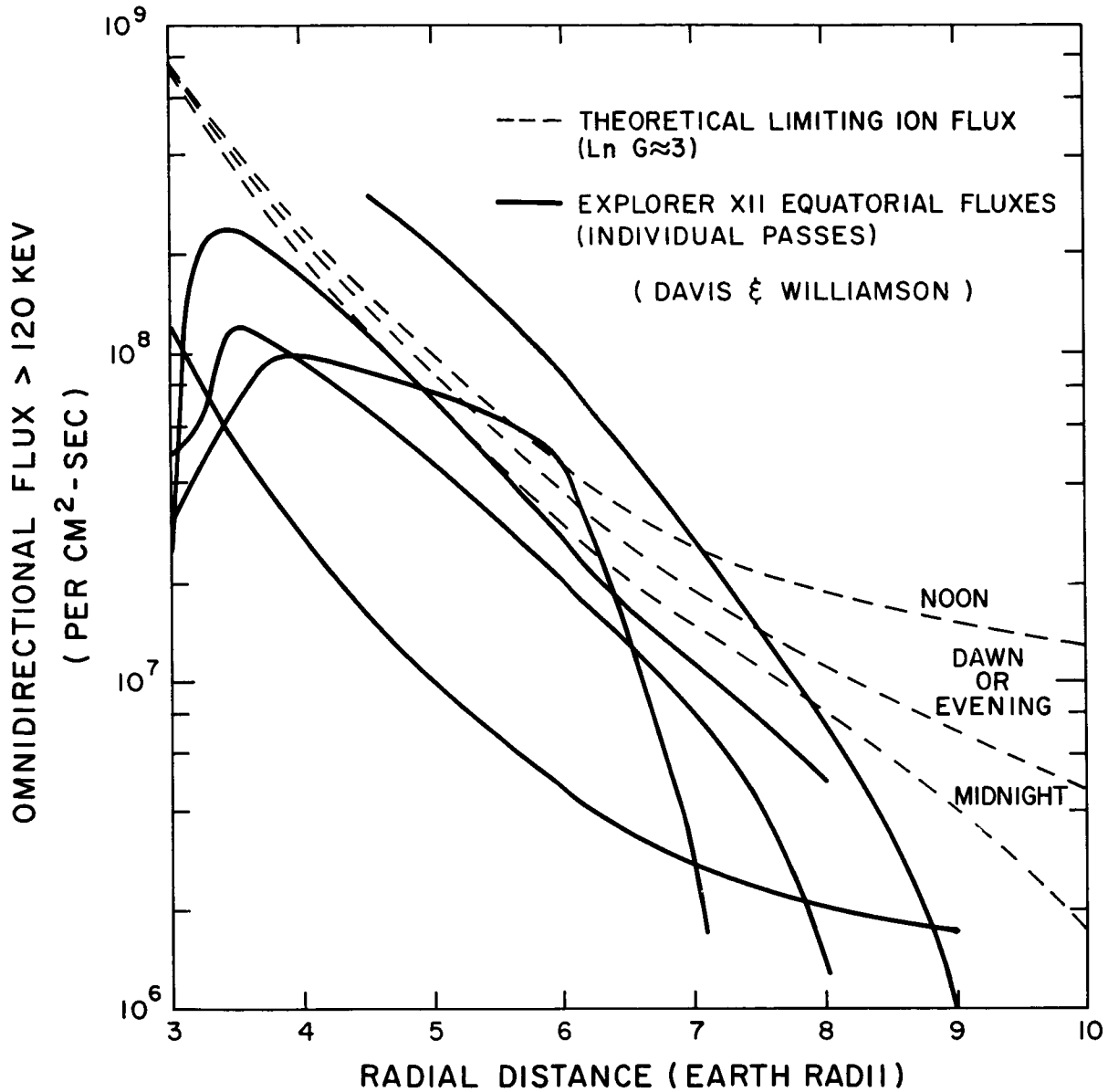
-52-

A4005

Fig. 12   Limitation on trapped protons. Here we have superposed
Explorer 12 radial distributions of trapped protons with
energies between 120 keV and 4.5 Mev and the theoretical
limiting protons flux J* (> 120 keV). For L > 4 it appears
that protons are also accelerated to their limiting fluxes.
These proton fluxes are comparable with the electron
fluxes of Figs. 10 and 11. Therefore energetic protons
can and often do have a much larger number density than
energetic electrons.

since the lower hybrid resonance reflects waves at intermediate latitudes, a very small fraction of the equatorial whistler amplitude should reach the ionosphere, where published observations by Injun III (Gurnett and O'Brien, 1964) were taken. Therefore, it is not surprising that their observed amplitudes were considerably smaller than those needed in the equatorial plane to account for Van Allen electron precipitation.

More recent measurements with the OGO-I satellite indicate that bursts of whistler radiation with wide band amplitudes the order of $10^{-2-3}\gamma$ in the equatorial plane are a reasonably common occurrence. (R. A. Helliwell, private communication.) Intermittent turbulence is to be expected since the trapped electron fluxes are more often than not below the instability limit and turbulence should occur only when there is a source of new cyclotron electrons. This noise appears to be limited to the Van Allen Zone, where the lines of force are topologically dipole. The amplitudes measured at intermediate latitudes, at most $\lambda \approx 50^{o}$ for OGO-I, were often comparable with those in the equatorial plane, suggesting, perhaps, that electron Landau damping was not active, at least at those times.

5.2d) Ion Cyclotron Wave Intensity

The precipitation rate of protons has, to our knowledge, not yet been satisfactorily measured. Nevertheless, Fig. 12 and Cornwall's (1966) results indicate that ion cyclotron instability must operate at least part of the time. Since we do not know the ion precipitation rate, we do not know the source strength of new protons driving the pitch angle diffusion.

We may estimate a lower limit for the equatorial plane ion cyclo-
tron wave intensity as follows: It is known that the lifetime of 60 keV pro-
tons against atmospheric charge exchange processes is roughly 6×10^5 sec
at $L \approx 6$. (Cornwall, 1966) When the ion cyclotron upper limit is obeyed,
the source strength and therefore the proton lifetime must be faster than
that given by charge exchange processes.

The lifetime T_L is related to the pitch angle diffusion coefficient
roughly as follows: (Kennel and Petschek, 1966)

$$T_L \sim 3/D^+ \tag{5.8}$$

and $D^+ \approx \Omega_+ \beta_\omega$ (Eq. 4.3). Substituting the charge exchange lifetime as a
lower limit, and taking $B_o \approx 200\gamma$ appropriate to $L \approx 6$, we find

$$B' > 10^{-1}\gamma \tag{5.9}$$

This estimate was first made by Cornwall (1966), using a variation upon
this reasoning.

In the absence of coordinated ray path and instability calculations,
it is not possible to estimate accurately the width of the region of high ion
cyclotron wave intensity near the equatorial plane. In addition, propagation
and absorption effects through the ionosphere make estimations of the wave
amplitudes in space using ground-based measurements, a subtle and compli-
cated procedure (Wentworth, 1964a and b). (5.9) does not disagree with
Wentworth's estimates. More recent low altitude satellite observations
from 1963 38C (Zmuda, et al, 1966) and OGO-II (Brody, et al, 1966) indicate
that extremely large amplitude $(30\gamma < B' < 300\gamma)$ transverse hydromagnetic
waves, with frequencies below the equatorial proton gyrofrequency, are observed

high altitudes, roughly corresponding to the high latitude border of the auroral electron precipitation zone. Thus, the connection with proton precipitation within the Van Allen Zone is at present unclear. Since the lowest intensity measurable by 1963 38C was 30γ, more sensitive measurements in the $1/10\gamma$ range may eventually clarify the situation. The OGO-II results indicated that the hydromagnetic emissions were often structured, rather than broad-band, indicating that a theoretical analysis more complete than that given here is needed for these observations.

6. Parasitic Diffusion

6.1) Parasitic Pitch Angle Diffusion

In this section we consider the possibility that the turbulent wave distributions created and maintained by the acceleration sources of, say, 40 keV cyclotron electrons and protons, drive precipitation of higher energy cyclotron particles as well. This can happen in at least two ways. First, the waves created at the equator can propagate into regions where the cyclotron resonant energies are higher than at the equator. Secondly, pitch angle diffusion at higher cyclotron resonances could also occur when the wave spectrum has a distribution of wave normal angles with respect to the magnetic field.

Referring to Table I of section 2, we see that the principal $n = \pm 1$ cyclotron resonant energies vary along a ray path as B^3/N for whistlers and for ion cyclotron waves as B^4/N. Therefore, these resonant particle energies increase rapidly upon leaving the equatorial plane. While these high energy off-plane resonant particles make a small contribution to the

overall growth rate, they will be scattered in pitch angle by whatever wave amplitude reaches high latitudes. If the wave energy density were constant going from the equatorial plane to the higher latitude scattering region, the ratio of the high latitude diffusion coefficient to that in the equatorial plane would be inversely proportional to the ratio of magnetic field strengths. Then the high latitude scattering rate for high energy particles would be reasonably fast. However, Landau damping cuts in, at least for whistlers, at latitudes above 8°, and the wave amplitudes should be diminished somewhat. At a latitude of 8° the dipole magnetic strength has only increased by a few percent and the cyclotron energies by 20%, relative to those in the equatorial plane. It is probably safe to say that cyclotron electrons with energies a factor two greater than those in the equatorial plane cannot be efficiently precipitated by off-plane whistler interactions. On the other hand, this conclusion depends strongly on the intensity of 100 eV Landau electrons.

We have directed our attention primarily to parallel propagating whistlers and ion cyclotron waves, and the electrons and ions resonant with them, as the most unstable, and contributing the lion's share to overall instability. However, especially when there are relatively few 100 eV Landau damping electrons, the wave spectrum in the equatorial plane turbulent region will have a spread of wave normal angles relative to the local magnetic field. Therefore, in addition to wave-particle interactions at the n = 0 Landau resonance already discussed, all the higher cyclotron resonance interactions ($|n| > 1$) are no longer forbidden when $K_\perp$ is nonzero. Kennel and Engelmann (1966) have shown that so long as the resonant

particle parallel velocity is much larger than the maximum parallel wave

phase velocity in the excited spectrum, the behavior of all higher cyclotron

resonances is similar to that of the principal $n = \pm 1$ cyclotron resonance

heretofore discussed. In other words, higher cyclotron harmonic diffusion

is almost purely in pitch angle and also leads to precipitation. The diffusion

rate will, in general, be slower since the wave particle coupling strength,

denoted by $|\vec{\theta}^{\pm}_{n,\underset{\sim}{K}}|^2$ in (4.1), is weaker for the higher cyclotron resonances.

Since the instability is caused by the $n = \pm 1$ principal resonance electrons,

the diffusion of the higher resonance electrons is, in some sense, gratuitous.

When the $n = \pm 1$ electrons approach their critical unstable intensity,

whistler instability occurs, scattering both $n = \pm 1$ and higher cyclotron

electrons in pitch angle. The higher cyclotron electrons need not be near

their limiting flux to be precipitated by whistler turbulence. However,

they do not, in general, limit their own intensities. For this reason, we

call this parasitic diffusion.

Figure 13 schematically illustrates parasitic diffusion. Shown is a

segment of $(V_\perp, V_{||})$ velocity space, with $V_{||} > 0$. This has negative $(n<0)$

cyclotron resonances with that part of the whistler spectrum with $\omega_{\underset{\sim}{K}}/K_{||} < 0$.

The $V_{||} < 0$ particles have negative cyclotron resonances with the opposite

half $\omega_{\underset{\sim}{K}}/K_{||} > 0$ of the whistler spectrum. The shaded regions indicate locations

in velocity space where the $n = -1$ principal cyclotron resonance diffusion

coefficient and the $n = -2$ parasitic diffusion coefficient are nonzero. The

picture could easily be extended to include all the $n = -3, -4 \ldots \ldots$ para-

sitic resonances. The $n = +1, +2, +3 \ldots$ resonances from the $\omega_{\underset{\sim}{K}}/K_{||} > 0$

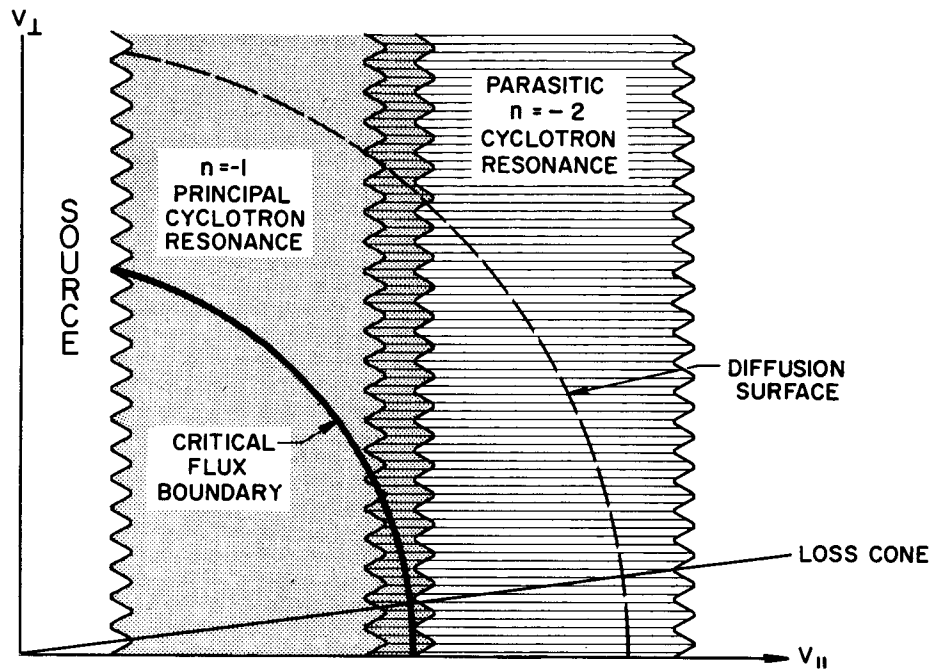half of the whistler spectrum approximately overlap the negative resonances

Fig. 13   Parasitic Pitch Angle Diffusion

Shown is a segment of the $(V_\perp V_{||})$ plane with shaded regions
where the diffusion coefficients from the overlapping n = -1
and n = -2 cyclotron resonances are non zero. A source,
here visualized at flat pitches, continually creates new high
energy particles which diffuse in pitch angle towards the
loss cone without changing much their energy. Those
particles which reach the loss cone within the n = -1
region are quickly precipitated and rapidly adjust their
intensities. Particles of slightly higher energy must use
the n = -2 diffusion band near the loss cone . While this
is a slow process, these particles will eventually be
precipitated. The n = -2 particles, because of their small
numbers, ordinarily do not contribute much to wave growth
rates.

A6675

from $\omega_K/K_{||} < 0$ waves shown, and so do not need to be explicitly drawn. They can alter only slightly the diffusion rate. The solid line shows the boundary in velocity space between the low energy cyclotron region where the distribution is near the critical intensity, and the high energy region, where intensities are well below critical. All electrons within this boundary can diffuse directly into the loss cone at the principal cyclotron resonance. Therefore, they adjust their numbers rapidly to keep the whistler distribution near marginal stability. Notice that to get efficiently into the loss cone, an electron must be in the principal resonance region near the loss cone as well as far away.

The dotted line shows a typical diffusion surface for those higher energy electrons whose intensity is below critical and which cannot therefore reach the loss cone via principal resonance diffusion alone. They do diffuse rapidly in the principal resonance region when their parallel velocity is small. In the absence of parasite resonances, however, they could never reach the loss cone.

When the wave distribution has a sufficiently broad spread in $K_{||}$, there can, in general, be an overlap region where particle diffuse with the sum of the principal and parasitic diffusion coefficients. In this way, a diffusion flux can penetrate the $n = -2$ parasitic region. What follows will be an extremely rough, schematic estimate of the diffusion rate in the $n = -2$ parasitic region for whistler-electron interactions. Since the same whistler distribution drives diffusion at both resonances, the relative diffusion rates can depend only on the ratio of weighting functions. These contain Bessel functions, whose arguments are

$$\frac{K_\perp V_\perp}{|\Omega_-|} \approx \frac{K_\perp}{K_{||}} \frac{V_\perp}{V_{||}} \frac{K_{||} V_{||}}{|\Omega_-|} \qquad (6.1)$$

From the resonance condition $K_{||}V_{||} = \omega - n\Omega_-$, we see that $K_{||}V_{||}/|\Omega_-| \approx n$, when $|\omega/\Omega_-| \ll 1$. Similarly we estimate $K_\perp/K_{||}$ by Θ, the wave normal angle to the magnetic field, and $V_\perp/V_{||}$ by a, the pitch angle. Thus

$$\frac{K_\perp V_\perp}{|\Omega_-|} \approx n\Theta a \tag{6.2}$$

With this crude approximation and the small argument expansions for Bessel function, we arrive at a simple estimate for the weighting functions $\left|\Theta^\pm_{n,\underset{\sim}{K}}\right|^2$ as a function of n. Here we tacitly assume that the equatorial plane whistler distribution, while having a spread of wave-normal angles is restricted to a reasonably small cone of angles about the magnetic field. When $n < 0$, we have

$$\left|\Theta^-_{n,\underset{\sim}{K}}\right|^2 \propto \frac{\left(\frac{|n|-1}{2}\Theta a\right)^{2|n|-2}}{(|n|-1)!} \tag{6.3}$$

Thus, when $n = -1$, $\left|\Theta^-_{-1,\underset{\sim}{K}}\right|^2 \sim 1$; for $n = -2$, $\left|\Theta^\pm_{-2,\underset{\sim}{K}}\right|^2 \sim (\Theta a/2)^2$, and so on. Since their weighting functions are small, higher cyclotron resonances only make small contributions to the growth rate at any point.

(6.3) permits an estimate of the parasitic pitch angle diffusion rates in various regions of velocity space. For instance, in the main part of the pitch angle distribution, where $a \simeq 1$, the parasitic pitch angle diffusion rate from a given wave depends only on its wave normal angle, Θ. The diffusion rate from all the waves will then depend roughly on the width of the excited wave distribution, which can in turn be estimated from the instability analysis, knowing the relative number of $n = 0$ Landau and $n = -1$ cyclotron electrons. Here the diffusion rate is moderately rapid.

However, the parasitic diffusion rate decreases with pitch angle. In fact, particles propagating exactly along the magnetic field, with $V_\perp = 0$, are not affected at all by parasitic pitch angle diffusion. It is clear that in diffusing by parasitic interactions from large pitch angles towards the loss cone, a particle spends most of its time near the loss cone. Thus, the lifetime will be dominated by the slow diffusion near the loss cone. A measure of the lifetime is thus the time T_n^* it takes a particle to diffuse the width of the loss cone at the rate given at the edge of the loss cone.

$$
T_n^* \sim \alpha_o^2 \left\{ \frac{\left(\frac{(n-1)}{2} \theta \alpha_o \right)^{2n-2}}{(n-1)!} \left| \Omega_- \middle| \beta_\omega \right| \right\}^{-1}
\tag{6.4}
$$

Here we have used the fact that the $n = -1$ diffusion coefficient is roughly $\left| \Omega_- \middle| \beta_\omega \right.$. The actual lifetime will probably be a few multiples of the basic time T_n^*. The $n = -2$ resonance lifetime, T_{-2}^*, is roughly independent of the size of the loss cone, while the higher resonances depend upon increasingly high powers of the loss cone size. Thus, high harmonic pitch angle diffusion should only be important on low L-shells, where the loss cone is reasonably large ($\alpha_o \sim 1/20$ radian at $L \sim 6$, $\alpha_o \sim 1/7$ radian at $L \sim 3$). In general, high harmonic parasitic diffusion is an inefficient way to precipitate high energy electrons using whistler interactions.

$n = -2$ parasitic diffusion may be able to explain some aspects of the precipitation of electrons of intermediate energy, 200-400 keV. Figure 14, taken from Williams and Smith (1964), shows lifetimes of electrons with energies $E_e > 280$ keV measured on the dayside of the Earth
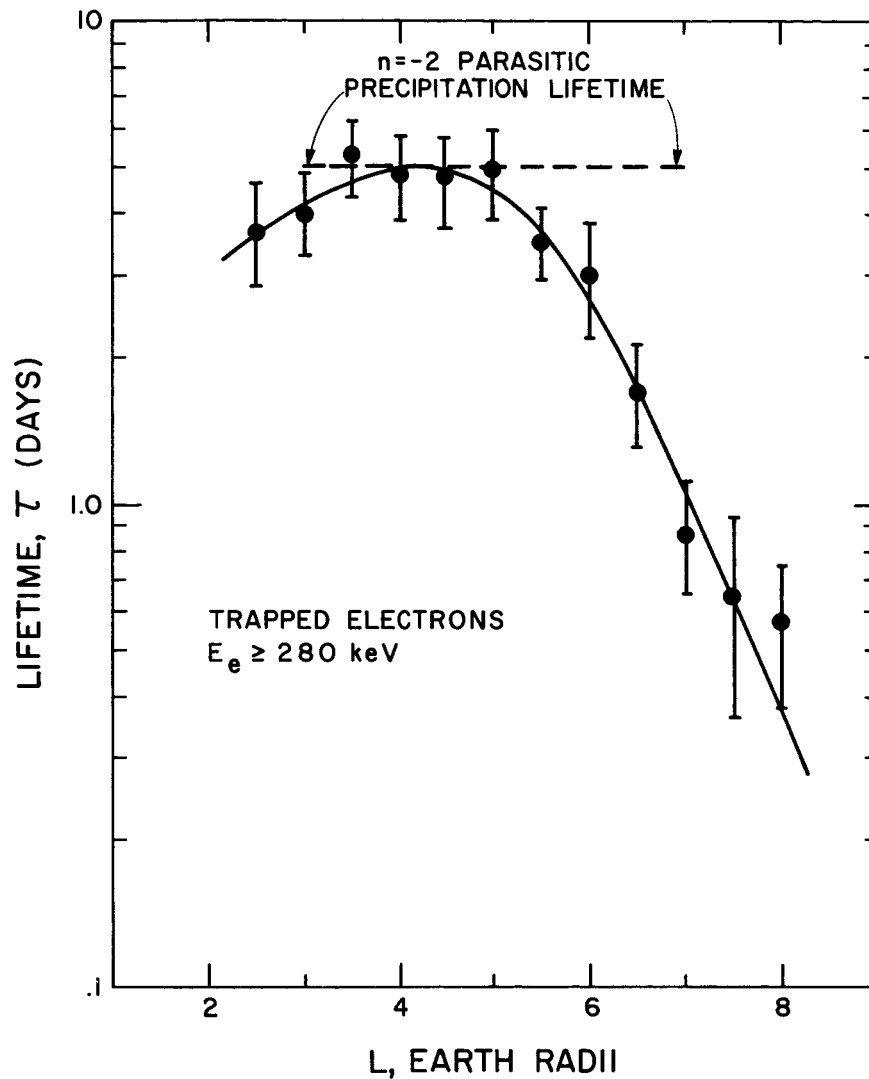
Fig. 14   Parasitic Precipitation Lifetimes for Electrons > 280 keV

We have superposed our estimate of the parasitic lifetimes
for electrons with energies > 280 keV upon the lifetimes
observed on the noon meridian by Williams and Smith (1964)
during a geomagnetically quite period. To arrive at this
estimate, we assumed that > 40 keV electrons were continually
precipitating with a lifetime of 10^4 seconds which was
independent of L. Electrons at L $\geq$ 6 probably intersect
the auroral zone and their lifetimes may be controlled by
the poorly understood processes occurring there.

A6717

with the satellite 1963 38C. The data were taken during a quiet time of relatively little magnetic activity. Injection of new electrons of this energy occurs only during magnetically disturbed times. The trapped fluxes were observed to decay in intensity with the plotted time constant. The observed intensity decay is quite likely due to diffusive precipitation. However, it cannot be from principal cyclotron resonance diffusion for two reasons. First of all, the fluxes observed were well below the critical flux for instability. Secondly, principal resonance precipitation, if source driven, would maintain a roughly constant intensity with time. A decaying trapped intensity cannot be due to $n = -1$ cyclotron diffusion. Suppose, however, that the low energy >40 keV electrons did have an acceleration source during the time of 1963 38C's observations. Kennel and Petschek (1966) argued that the critical flux boundary typically lies somewhere between 40 and 230 keV. Suppose it is at 100 keV typically; then 1963 38C's electrons can only penetrate the loss cone via the $n = -2$ parasitic resonance. O'Brien (1962) concluded that the average >40 keV electron lifetime is roughly constant with L , approximately 10^4 seconds, give or take a factor of 5 . The instability calculations outlined in section 3 suggest that the equatorial plane wave spectrum may have a width of $\Theta \sim 1/3$ radian. Thus, from (6.4) we find:

$$T^*_{-2} \sim 4 \times 10^5 \text{ seconds} \approx 5 \text{ days} \tag{6.5}$$

This is in rough agreement with Williams and Smith's observations for the heart of the Van Allen Zone, $2 \leqslant L \leqslant 5$. However, for $L > 5$, some other more powerful precipitation mechanism intervenes. It should be noted

that the $L > 5$ electrons will intersect the auroral zone as they drift from the dayside, where the above observations were made, to the night side. Strong, but poorly understood, turbulence is known to occur in the auroral zone (O'Brien and Taylor, 1964). The lack of variation of the >280 keV electron lifetime with L in the Van Allen Zone is consistent with the constancy with L of the >40 keV lifetime and the fact that the $n = -2$ harmonic lifetime is independent of the loss cone size.

We summarize the properties of cyclotron harmonic parasitic precipitation as follows: It occurs when lower energy particles have an acceleration source, are themselves precipitating, and are consequently limited at the critical flux. The parasitic lifetimes are longer than the principal lifetimes, and depend upon the width α_o of the loss cone and the angular width of the wave spectrum. This last depends upon the relative numbers of low energy $n = 0$ Landau and $n = -1$ principal cyclotron particles. While we have discussed only the whistler mode, it is clear that analogous arguments are valid for parasitic proton precipitation via ion cyclotron turbulence.

Thus far, we have taken into account only the particle species which make the dominant contribution to the overall growth rate: electrons for whistlers, ions for the ion cyclotron waves. Clearly, the sub-dominant species, ions for whistlers, electrons for the ion cyclotron mode, can be resonantly scattered in velocity space by the existing turbulence even when they do not make a significant contribution to the growth rate. From Table I, we note that high energy electrons of a few meV energy could be scattered in pitch angle by ion cyclotron wave interactions. Thus, we expect a correlation between proton precipitation and relativistic electron precipitation, since high harmonic whistler diffusion is probably quite inefficient for electrons of relativistic energies.

6.2) Parasitic Landau Diffusion

As we have argued, diffusion at the Landau resonance is purely in the $V_{||}$ variable. If this diffusion were rapid, any damping $V_{||}$ gradients in the distribution functions could rapidly smooth out as well, reducing the net Landau damping. We may crudely estimate this rate by setting $n = 0$ in the whistler-electron coupling function.

$$\left| \Theta_{o,\underset{\sim}{K}}^{-} \right|^2 \propto \frac{J_1^2}{4} \left(\frac{K_\perp V_\perp}{|\Omega_-|} \right) \tag{6.6}$$

Analogously to (6.1), we estimate for the Landau resonance:

$$\frac{K_\perp V_\perp}{|\Omega_-|} \sim \frac{K_\perp}{K_{||}} \frac{V_\perp}{V_{||}} \frac{K_{||}V_{||}}{|\Omega_-|} \sim \Theta a \left| \frac{\omega}{\Omega_-} \right| \tag{6.7}$$

Thus,

$$\left| \Theta_{o,\underset{\sim}{K}}^{-} \right|^2 \sim \frac{1}{4} \left(\frac{\Theta a}{2} \frac{\omega}{\Omega_-} \right)^2 \tag{6.8}$$

When $\Theta \left| \omega/\Omega_- \right| \ll 1$, the Landau diffusion rate is much smaller than the principal cyclotron diffusion rate. During one cyclotron electron lifetime, the Landau electrons are hardly affected by the equatorial plane whistler turbulence, when Θ is small. If the source driving the turbulence lasts many cyclotron particle lifetimes, the Landau electrons eventually would smooth out due to whistler turbulence. When most of the whistlers propagate primarily across the field, the Landau diffusion rate could be comparable with or larger than the cyclotron diffusion rates. This might occur at high latitudes.

7. Discussion and Summary

7.1) Electrostatic Turbulence

We have discussed thus far the turbulence arising only from two of the three linear wave branches of plasmas, omitting the electrostatic branch of oscillations -- ion-sound waves and plasma oscillations. By the general arguments of section 4, when $\omega/\Omega_{\pm} \ll 1$, cyclotron resonances with electrostatic modes will also produce the almost pure pitch angle diffusion apparently required by observation. Consider the ion sound wave, which has a maximum phase velocity parallel to B_o of $(T-/M+)^{1/2}$, where $T-$ is the electron temperature and $M+$ the ion mass. Then the parallel energy of electrons in cyclotron resonance with the ion sound wave is:

$$\frac{1}{2} M_- \left(\frac{\omega}{K_{\|}}\right)^2 \left(1 - \frac{n\Omega_-}{\omega}\right)^2 \approx n^2 \left(\frac{\Omega_-}{\omega}\right)^2 \frac{1}{2} M_- \frac{T-}{M+} \approx \frac{n^2}{2} \left(\frac{\Omega_+}{\omega}\right)^2 \frac{M+}{M-} T- \qquad (7.1)$$

Thus, since $T- \approx 2$ eV (Serbu and Maier, 1966) ion sound waves with $\omega/\Omega_+ \sim 1/5$ resonate with ≈ 40 keV Van Allen electrons. Unlike for electromagnetic waves, pitch angle instabilities destabilize ion sound waves which propagate preferentially <u>across</u> the magnetic field. Moreover, the coupling to Landau particles is strong, and heavy Landau damping would seem at least intuitively to dominate the cyclotron instability from the trapped particle distribution. However, in view of the fact that Scarf, et al (1966) have observed large amplitude ion sound waves with frequencies comparable with the local ion gyrofrequency near and above the ionosphere, the relation of this upper ionospheric electro-static turbulence to trapped energetic particles mirroring there should be more precisely evaluated. At the very least, when a beam or current driven ion sound instability does occur, parasitic cyclotron electron precipitation could take place.

Another form of electrostatic turbulence can be created by the existence of the loss cone itself. (Rosenbluth and Post, 1965; Post and Rosenbluth, 1966). An analysis of this instability, tailored to the magnetosphere, has been performed by Pearlstein, et al (1966). However, when the equatorial region of wave growth is sufficiently long, the whistler and ion cyclotron instability both easily have lower particle intensity thresholds than the ion and electron versions of the loss cone instability (Kennel, 1966; Kennel and Wong, 1966). As a general rule, the closeness of the observed electron and ion fluxes to the calculated upper limits set by whistler and ion cyclotron instability suggests that other "critical flux" instabilities rarely dominate the electromagnetic wave instabilities considered in this paper.

6.2) Precipitation from Enhanced Fluctuations in Non-Thermal Stable Plasmas

Thus far we have treated pitch angle scattering only from unstable plasma turbulence. However, when the velocity distributions are stable but have a high energy tail, the fluctuating field levels can be much higher than in thermal equilibrium, with a corresponding enhanced wave-particle scattering rate. This possibility was evaluated for the Van Allen Belts by Eviatar (1966), who calculated a lifetime of 5×10^4 seconds using stable but enhanced ion sound fluctuations arising from the observed Van Allen high energy electrons. We argued in section 5 that similar effects should also occur for electromagnetic waves, which, as we have shown, hover near marginal stability.

6.3) Summary

The work outlined in this paper is an attempt to apply the basic philosophy and methods of the rapidly developing fields of weak plasma

turbulence to the plasmas in space near the Earth. While many points need to be filled in and clarified, it does seem that a reasonable case can be made that pitch angle diffusion driven by whistler and ion cyclotron turbulence precipitates particles from the magnetosphere to the atmosphere, thereby fixing an upper limit to stably trapped particle intensities. When as yet unspecified acceleration sources keep the fluxes near their critical intensities, pitch angle scattering from turbulence in these modes appears, from the experimental evidence, to dominate all others, driving both the primary low energy particles and, possibly, secondary intermediate energy particles out of the Earth's mirror field. This only means, of course, that cyclotron fluxes are often forced below critical. Then other mechanisms, some of which were briefly mentioned here, must dominate the physics, since whistler and ion cyclotron turbulence cannot occur.

Although an enormous number of interesting geophysical experiments and observations have been performed, our understanding of them, at a deep plasma physical level, is still relatively rudimentary. At the risk of sounding hopelessly dated a few years hence, we should like now to discuss a few of the more intriguing unsolved problems. First of all, what is the origin of the intense non-steady structured turbulent noise and particle precipitation phenomena, noted by many observers, whose importance has been emphasized by Cornwall (1966)? In the case of whistlers, there is evidence that intense structured emissions can be stimulated by man-made signals (Helliwell, et al, 1964). It appears that the man-made signals from the ground must have a duration of greater than 10^{-1} seconds to stimulate the magnetospheric emissions. In general, the stimulated whistler frequency increases with time, though falling tones are also sometimes observed.

For further discussion of these and other structured whistler noise bursts, see Brice (1964). Since the time scale of structured emission is comparable with particle bounce periods, and since the distribution of waves in K-space is inhomogenous and time-varying, the rough methods outlined here which average over all such effects, are not adequate to explain structured whistler and ion cyclotron emissions.

Another area open for investigation is that of acceleration of particles to high energies. Acceleration mechanisms apparently do exist, but what exactly they are is a mystery. One acceleration mechanism, involving the violation of the third invariant during those periods of whistler and ion cyclotron stability when the first adiabatic invariant is surely conserved has been proposed by Nakada, et al (1965). The electric fields associated with slow changes in the Earth's magnetic field, caused by, for instance, fluctuations in the solar wind, cause particles to walk gradually inwards towards the Earth. Because they conserve their first adiabatic invariant, their energy increases as they penetrate regions of increasing magnetic field strength. Whether or not this source accounts for the general day-to-day precipitation levels in the Van Allen Belts remains to be seen. The intense >40 keV electron precipitation observed by O'Brien (1964) on night side auroral lines of force probably corresponds to a lifetime shorter than the electrons' drift period about the Earth. Thus, third adiabatic acceleration may not be able to provide a strong enough source to account for all precipitation observations.

Finally, the intense activity in the auroral zone remains to be understood. Axford, et al (1965) have demonstrated that the plasma flow

from the neutral sheet in the magnetospheric tail into the auroral zone on the Earth's night side transports sufficient particle energy to account for all the auroral and Van Allen dissipation. In this case, a possible source of ≈ 1 keV plasma to drive auroral zone turbulence could simply be plasma injection from the magnetospheric tail. The relationship of this source to the intense auroral precipitation, to the possible acceleration of high energy particles, and to the highly localized, intense auroral arcs is at present unclear. However, these and many other fascinating topics are under active scrutiny at this time and we confidently expect rapid progress and many surprises in the near future.

ACKNOWLEDGMENTS

REFERENCES

Allis, W.P., S.J. Buchsbaum, and A. Bers, Waves in anisotropic plasmas, MIT Press, 1963.

Anderson, K.A. and D.W. Milton, Balloon observations of X rays in the auroral zone, 3, High time resolution studies, J. Geophys. Res., 69 (21), 4457-4480, 1964.

Andronov, A.A., and V.V. Trakhtengerts, Kinetic instability of the earth's outer radiation belt, English Transl., Geomagnetism and Aeronomy, 4, (2), 181, 1964.

Angerami, J., and D. Carpenter, Whistler studies of the plasmapause in the magnetosphere, 2, Electron density and total tube electron content near the knee in magnetospheric ionization, J. Geophys. Res. 71, 3, 711-726, 1966.

Axford, W.I., H.E. Petschek, and G.L. Siscoe, Tail of the magnetosphere, J. Geophys. Res., 70(5), 1231-1236, 1965.

Bame, S.J., J.R. Asbridge, H.E. Felthauser, R.A. Olsen, and I.B. Strong, Electrons in the plasma sheet of the earth's magnetic tail, Phys. Rev. Letters, 16, 138, 1966.

Berk, H.L., C.W. Horton, M.N. Rosenbluth, and R.N. Sudan, Plasma wave reflection in slowly varying media, ICTP Trieste Preprint IC/66/93.

Brice, N.M., Fundamentals of very low frequency emission generation mechanisms, J. Geophys. Res., 69 (21), 4515-4522, 1964.

Brice, N.M., Discrete VLF emissions from the upper atmosphere, Stanford University Technical Report 3412-6 (SU-SEL-64-088), 1964.

Bridge, J., A. Egidi, A. Lazarus, E. Lyon and L. Jacobson, Preliminary results of plasma measurements on Imp A, COSPAR Preprint, Florence, Italy, May, 1964.

Brody, K. I., R.E. Holzer, and E. J. Smith, Observations of magnetic fluctuations on the OGO 2 satellite, TRANS. AGU, 47, 463, 1966, (abstract).

Brown, R. R., Electron precipitation in the auroral zone, Space Science Reviews, 5, 311-387, 1966.

Cahill, L. J. and P. J. Amazeen, The boundary of the geomagnetic field, J. Geophys. Res., 68, 1835-1844, 1963.

Camac, M., A. R. Kantrowitz, M. M. Litvak, R. M. Patrick, and H. E. Petschek, Shock waves in collision free plasmas, Nucl. Fusion Suppl., part 2, pp. 423-446, 1962.

Carpenter, D., Whistler studies of the plasmapause in the magnetosphere, 1, Temporal variations in the position of the knee and some evidence of plasma motions near the knee, J. Geophys. Res. 71, 3, 693-710, 1966.

Carpenter, D. L., and R. L. Smith, Whistler measurements of electron density in the magnetosphere, Rev. Geophys. 3, 415-441, 1964.

Cornwall, J. M., Scattering of energetic trapped electrons by very-low-frequency waves, J. Geophys. Res., 69, 1251-1258, 1964.

Cornwall, J. M., Cyclotron instabilities and electromagnetic emission in the ultralow frequency and very low frequency ranges, J. Geophys. Res., 70 (1), 61-70, 1965.

Cornwall, J. M., Micropulsations and the outer radiation zone, J. Geophys. Res. 71, 9, 2185-2200, 1966.

Davis, L. R. and J. M. Williamson, Low-energy trapped protons, Space Res., 3, 365-375, 1963.

Dessler, A. J., and R. D. Juday, Configuration of auroral radiation in space, Planet. Space Sci., 13, 63-72, 1965.

Dragt, A. J., Effect of hydromagnetic waves on the lifetimes of Van Allen radiation protons, J. Geophys. Res., 66, 1641-1649, 1961.

Drummond, W. E., and D. Pines, Nonlinear stability of plasma oscillations, Nucl. Fusion Suppl., part 3, pp. 1049-1058, 1962.

Dungey, J. W., Loss of Van Allen electrons due to whistlers, Planetary Space Sci., 11, 591-595, 1963.

Dungey, J. W., Effects of Electromagnetic perturbations on particles trapped in the radiation belts, " Space Sci. Rev. 4, 199-222, 1965.

Eviatar, A., The role of electrostatic plasma oscillations in electron scattering in the earth's outer magnetosphere, J. Geophys. Res., 71, 11, 2715-2728, 1966.

Fishman, F. J., A. R. Kantrowitz, and H. E. Petschek, Magneto-hydrodynamic shock wave in a collision-free plasma, Rev. Mod. Phys. 32, 959-966, 1960.

Frank, L. A., A survey of electrons E > 40 kev beyond 5 earth radii with Explorer 14, J. Geophys. Res., 70(7), 1593-1626, 1965.

Fritz, T. A., and D. A. Gurnett, Diurnal and latitudinal effects observed for 10 kev electrons at low satellite altitudes, J. Geophys. Res., 70, 2485-2502, 1965.

Galeev, A. A., Ion Escape from a magnetic mirror trap due to development of instability connected with the loss cone, " Sov. Phys. (English Trans.) JETP 22, 466-472, 1966

Galeev, A. A., and V. I. Karpman, Turbulence theory of a weakly nonequilibrium low density plasma and structure of shock waves, Sov. Phys. JETP, 17, 2, 403-409, 1963.

Gurnett, D. A., and B. J. O'Brien, High-latitude studies with satellite Injun 3, 5, Very low frequency electromagnetic radiation, J. Geophys. Res. 69(1), 65-90, 1964.

Haerendel, G., On the violation of the second and third adiabatic invariants, J. Geophys. Res., 71, 1857-1868, 1966.

Helliwell, R. A., Whistlers and related ionospheric phenomena, Stanford Press, 1965.

Helliwell, R. A., J. Katsufrakis, M. Trimpi, and N. Brice, Artificially stimulated very low frequency radiation from the ionosphere, J. Geophys. Res., 69, 2391-2394, 1964.

Kantrowitz, A. R., and H. E. Petschek, MHD characteristics and shock waves, Plasma Physics in Theory and Application, Ed. by Wulf B. Kunkel, McGraw-Hill Book Co, New York, 1966.

Kennel, C. F., Low Frequency Whistler Mode, Phys. Fluids, 9, 11, 1966.

Kennel, C. F., and F. Engelmann, Velocity space diffusion from weak plasma turbulence in a magnetic field, Phys. Fluids, 9, 12, 1966.

Kennel, C. F., and H. E. Petschek, A limit on stably trapped particle fluxes, J. Geophys. Res., 71, 1, 1-28, 1966.

Kennel, C. F., and R. M. Thorne, Unstable growth of unducted whistlers propagating at an angle to the geomagnetic field (to be published in J. Geophys. Res.) June 1966.

Kennel, C. F. and H. V. Wong, Resonant particle instabilities in a uniform magnetic field (to be published)

Kennel, C. F. and H. V. Wong, Resonantly unstable off-angle hydromagnetic waves, J. Plasma Physics, 1, 1, 1967.

Kimura, I., Effects of ions on whistler mode ray tracing, Radio Science, 1, 3, 269-283, 1966.

Levy, R. H., H. E. Petschek, and G. L. Siscoe, Aerodynamic aspects of the magnetospheric flow, AIAA J. 2:2065-2076, 1964.

Liemohn, H. B., Cyclotron Resonance Amplification of VLF and ULF whistlers, (to be published in J. Geophys. Res.).

Lyon, E. F., Explorer 18 plasma measurements, in The Solar Wind R. J. Mackin and M. Neusebauer, eds., Pergamon Press, Oxford, 1966, pp. 295-314.

McDiarmid, I. B., and E. E. Budzinski, Angular distributions and energy spectra of electrons associated with auroral events, Can. J. Phys., 42 (11), 2048-2062, 1964.

McDiarmid, I. B., J. R. Burrows, E. E. Budzinski, and M. D. Wilson, Some average properties of the outer radiation zone at 1000 km, Can J. Phys., 41, 2064-2079, 1963.

McDiarmid, I. B., and J. R. Burrows, Electron fluxes at 1000 kilometers associated with the tail of the magnetosphere, J. Geophys. Res. 70, 3031-3044, 1965.

Mozer, F. S., Rocket measurements of energetic particles, 2, Electron results, J. Geophys. Res., 70, 5709-5716, 1965.

Mozer, F. S., J. F. Crifo, and J. E. Blamont, Rocket Measurements of energetic particles, 1, Description of the experiment, J. Geophys. Res. 70, 5699-5707, 1965.

Mozer, F. S. and P. Bruston, Properties of the auroral zone electron source deduced from electron spectrums and angular distributions, J. Geophys. Res., 71, 4451-4460, 1966.

Mozer, F. S. and P. Bruston, Auroral zone proton-electron anticorrelation, proton angular distributions, and electric fields, J. Geophys. Res., 71, 4461-4468, 1966.

Nakada, M. P., J. W. Dungey, and W. N. Hess, On the origin of outer belt protons, J. Geophys. Res., 70, 3529-3532, 1965.

Ness, N. F., The earth's magnetic tail, J. Geophys. Res., 70, 2989-3006, 1965.

Ness, N. F., Observations of the solar wind interaction with the geomagnetic field: Conditions quite, NASA document X-612-66-381, 1966.

Ness, N. F., C. S. Scearce and J. B. Seek, Initial results of the Imp 1 magnetic field experiment, J. Geophys. Res., 69, 17, 3531-3569, 1964.

O'Brien, B. J., Lifetimes of outer-zone electrons and their precipitation into the atmosphere, J. Geophys. Res., 67, 3687-3706, 1962.

O'Brien, B. J., High latitude geophysical studies with satellite Injun 3, 3, Precipitation of electrons into the atmosphere, J. Geophys. Res. 69(1), 13-44, 1964.

O'Brien, B. J., Interrelations of energetic charged particles in the magnetosphere, Rice University Space Sciences Preprint, to be published in the proceedings of the Inter-Union Symposium on Solar Terrestrial Physics, Belgrade, Yugoslavia, Aug. 29-Sept. 2, 1966.

O'Brien, B. J. and Taylor, H., High latitude geophysical studies with satellite Injun 3, 4. Auroras and their excitation, J. Geophys. Res. 69, 1, 45-64, (1964).

Pearlstein, L. D., M. N. Rosenbluth, and D. B. Chang, High frequency "Loss-Cone" flux instabilities inherent to two-compoent plasmas, Phys. Fluids 9, 953-955, 1966.

Post, R. F. and M. N. Rosenbluth, Electrostatic instabilities in finite mirror confined plasmas, Phys. Fluids 9, 730-749, 1966.

Rosenbluth, M. N., and R. F. Post, High frequency electrostatic plasma instability inherent to "Loss-Cone" particle distributions, Phys. Fluids 8, 547-550, 1965.

Sagdeev, R. Z., and V. D. Shafronov, On the instability of a plasma with an anisotropic distribution of velocities in a magnetic field, Soviet Physics, JETP English Transl., 12(1), 130-132, 1961.

Scarf, F. L., G. M. Crook, and R. W. Fredricks, Preliminary report on detection of electrostatic ion waves in the magnetosphere, " J. Geophys. Res. 70, 3045-3060, 1965.

Serbu, G. P., and E. J. R. Maier, Low energy electrons measured on Imp 2, J. Geophys. Res. 71, 15, 3755-3766, 1966.

Stix, T. H., The Theory of Plasma Waves, Mc-Graw-Hill Book Company, New York, 1962.

Stix, T.H., Radiation and absorption via mode conversion in an inhomogenous collisionfree plasma, Phys. Rev. Letters, 15, 878-882, 1965.

Thorne, R.M. and C.F. Kennel, Quasi-trapped VLF propagation in the outer magnetosphere, Avco Everett Research Report 251, 1966, to be published in J. Geophys. Res.

Van Allen, J.A., First public lecture on the discovery of geomagnetically trapped radiation, transcript of remarks as delivered on May 1, 1958, to the National Academy of Sciences, Washington, D.C., IGY Satellite Report #13, Jan. 1961, IGY World Data Center A, Rockets and Satellites, National Academy of Sciences, National Research Council.

Vedenov, A.A., E.P. Velikhov, and R.Z. Sagdeev, Quasi-linear theory of plasma oscillations, Salzburg, 1961; Nucl. Fusion Suppl., 2, 465-475, 1962.

Watanabe, T., Determination of the Electron Distribution in the magnetosphere using hydromagnetic whistlers, J. Geophys. Res. 70, 5839-5848 (1965).

Wentzel, D.G., Hydromagnetic waves and trapped radiation, 1, Breakdown of the adiabatic invariance; 2, Displacement of the mirror points, J. Geophys. Res., 66, 359-362, 363-369, 1961.

Wentworth, P.C., Evidence for maximum production of hydromagnetic emissions above the afternoon hemisphere of the earth, 1, Extrapolation to the base of the exosphere, 2, Analysis of statistical studies, J. Geophys. Res., 69, 2689-2698, 2699-2706, 1964.

Williams, D.J. and A.M. Smith, Daytime trapped electron intensities at high latitudes at 1000 kilometers, J. Geophys. Res., 70, 541-556, 1965.

Winckler, J.R., P.D. Bhavsar, and K.A. Anderson, A study of the precipitation of energetic electrons from the geomagnetic field during magnetic storms, J. Geophys. Res., 67, 3717-3736, 1962.

Wolfe, J.H., R.W. Silva, and M.A. Myers, Observations of the solar wind during the flight of Imp I, J. Geophys. Res., 71, 1319-1340, 1966.

Zmuda, A.J., J.H. Martin, and F.T. Heuring, Transverse hydromagnetic disturbances at 1100 km in the auroral region, J. Geophys. Res., 71, 5033-5046, 1966.

DOCUMENT CONTROL DATA - R&D

(Security classification of title body of abstract and indexing annotation must be entered when the overall report is classified)

1 ORIGINATING ACTIVITY (Corporate author)	2a REPORT SECURITY CLASSIFICATION
Avco Everett Research Laboratory 2385 Revere Beach Parkway Everett, Massachusetts	Unclassified
	2b GROUP

3 REPORT TITLE

VAN ALLEN BELT PLASMA PHYSICS

4 DESCRIPTIVE NOTES *(Type of report and inclusive dates)*

Research Report 259

5 AUTHOR(S) *(Last name, first name, initial)*

Kennel, C. F., and Petschek, H. E.

6. REPORT DATE	7a. TOTAL NO. OF PAGES	7b. NO. OF REFS
December 1966	77	79

8a. CONTRACT OR GRANT NO. AF 49(638)-1483 b. PROJECT NO. c. d.	9a. ORIGINATOR'S REPORT NUMBER(S) Research Report 259 9b. OTHER REPORT NO(S) *(Any other numbers that may be assigned this report)*

10. AVAILABILITY/LIMITATION NOTICES

Qualified requesters may obtain copies of this report from DDC.

11. SUPPLEMENTARY NOTES	12. SPONSORING MILITARY ACTIVITY Department of the Air Force, AF Office of Scientific Research, Office of Aerospace Research, Arlington, Va.

13 ABSTRACT

We review recent theoretical developments in understanding the plasma turbulence in the Van Allen belts. More complex geophysical turbulence phenomena, such as the auroral zone, are not explicitly treated, since their theoretical description is still incomplete. In particular, it now appears likely that instability, and the resulting quasi-linear pitch angle scattering, in the so-called whistler and ion cyclotron modes, limits the fluxes of energetic electrons and ions, respectively, that can be stably trapped in the Van Allen belts, where the Earth's magnetic lines have a dipole "mirror" configuration. We discuss semi-quantitatively the factors which affect the stability of such waves propagating obliquely to the local magnetic field direction, the velocity space diffusion resulting from their nonlinear growth, and finally, some observations relating to the Van Allen belt turbulence.

(U)

DD FORM 1 JAN 64 **1473**

KEY WORDS	LINK A		LINK B		LINK C	
	ROLE	WT	ROLE	WT	ROLE	WT
1. Plasma turbulence 2. Van Allen belts 3. Trapped particles 4. Whistler mode 5. Pitch Angle scattering						

INSTRUCTIONS

1. ORIGINATING ACTIVITY: Enter the name and address of the contractor, subcontractor, grantee, Department of Defense activity or other organization (corporate author) issuing the report.

2a. REPORT SECURITY CLASSIFICATION: Enter the overall security classification of the report. Indicate whether "Restricted Data" is included. Marking is to be in accordance with appropriate security regulations.

2b. GROUP: Automatic downgrading is specified in DoD Directive 5200.10 and Armed Forces Industrial Manual. Enter the group number. Also, when applicable, show that optional markings have been used for Group 3 and Group 4 as authorized.

3. REPORT TITLE: Enter the complete report title in all capital letters. Titles in all cases should be unclassified. If a meaningful title cannot be selected without classification, show title classification in all capitals in parenthesis immediately following the title.

4. DESCRIPTIVE NOTES: If appropriate, enter the type of report, e.g., interim, progress, summary, annual, or final. Give the inclusive dates when a specific reporting period is covered.

5. AUTHOR(S): Enter the name(s) of author(s) as shown on or in the report. Enter last name, first name, middle initial. If military, show rank and branch of service. The name of the principal author is an absolute minimum requirement.

6. REPORT DATE: Enter the date of the report as day, month, year; or month, year. If more than one date appears on the report, use date of publication.

7a. TOTAL NUMBER OF PAGES: The total page count should follow normal pagination procedures, i.e., enter the number of pages containing information.

7b. NUMBER OF REFERENCES: Enter the total number of references cited in the report.

8a. CONTRACT OR GRANT NUMBER: If appropriate, enter the applicable number of the contract or grant under which the report was written.

8b, 8c, & 8d. PROJECT NUMBER: Enter the appropriate military department identification, such as project number, subproject number, system numbers, task number, etc.

9a. ORIGINATOR'S REPORT NUMBER(S): Enter the official report number by which the document will be identified and controlled by the originating activity. This number must be unique to this report.

9b. OTHER REPORT NUMBER(S): If the report has been assigned any other report numbers (either by the originator or by the sponsor), also enter this number(s).

10. AVAILABILITY/LIMITATION NOTICES: Enter any limitations on further dissemination of the report, other than those imposed by security classification, using standard statements such as:

(1) "Qualified requesters may obtain copies of this report from DDC."

(2) "Foreign announcement and dissemination of this report by DDC is not authorized."

(3) "U. S. Government agencies may obtain copies of this report directly from DDC. Other qualified DDC users shall request through

_____."

(4) "U. S. military agencies may obtain copies of this report directly from DDC. Other qualified users shall request through

_____."

(5) "All distribution of this report is controlled. Qualified DDC users shall request through

_____."

If the report has been furnished to the Office of Technical Services, Department of Commerce, for sale to the public, indicate this fact and enter the price, if known.

11. SUPPLEMENTARY NOTES: Use for additional explanatory notes.

12. SPONSORING MILITARY ACTIVITY: Enter the name of the departmental project office or laboratory sponsoring (paying for) the research and development. Include address.

13. ABSTRACT: Enter an abstract giving a brief and factual summary of the document indicative of the report, even though it may also appear elsewhere in the body of the technical report. If additional space is required, a continuation sheet shall be attached.

It is highly desirable that the abstract of classified reports be unclassified. Each paragraph of the abstract shall end with an indication of the military security classification of the information in the paragraph, represented as (TS), (S), (C) or (U).

There is no limitation on the length of the abstract. However, the suggested length is from 150 to 225 words.

14. KEY WORDS: Key words are technically meaningful terms or short phrases that characterize a report and may be used as index entries for cataloging the report. Key words must be selected so that no security classification is required. Identifiers, such as equipment model designation, trade name, military project code name, geographic location, may be used as key words but will be followed by an indication of technical context. The assignment of links, rules, and weights is optional